Studies on the role of disturbed Ca^{2+} homeostasis in the pathomechanism of the cardiac effects of experimental diabetes using conventional and novel experimental techniques

PhD Thesis

János Prorok, *MSc*

Department of Pharmacology & Pharmacotherapy
Albert Szent-Györgyi Medical Center
University of Szeged
Szeged, Hungary

2013

PUBLICATION LIST

a.) Published literature related to PhD topic

I. **Prorok J**, Kovács PP, Kristóf AA, Nagy N, Tombácz D, Tóth JS, Ordög B, Jost N, Virág L, Papp JG, Varró A, Tóth A, Boldogkoi Z. Herpesvirus-mediated delivery of a genetically encoded fluorescent $Ca(^{2+})$ sensor to canine cardiomyocytes. J Biomed Biotechnol. 2009;2009:361795. **IF: 1.770**

II. Birinyi P, Tóth A, Jóna I, Acsai K, Almássy J, Nagy N, **Prorok J**, Gherasim I, Papp Z, Hertelendi Z, Szentandrássy N, Bányász T, Fülöp F, Papp JG, Varró A, Nánási PP, Magyar J. The Na^+/Ca^{2+} exchange blocker SEA0400 fails to enhance cytosolic Ca^{2+} transient and contractility in canine ventricular cardiomyocytes. Cardiovasc Res. 2008 Jun 1;78(3):476-84. **IF: 5.947**

b.) Other studies

I. Nagy N, Szuts V, Horváth Z, Seprényi G, Farkas AS, Acsai K, **Prorok J**, Bitay M, Kun A, Pataricza J, Papp JG, Nánási PP, Varró A, Tóth A. Does small-conductance calcium-activated potassium channel contribute to cardiac repolarization? J Mol Cell Cardiol. 2009 Nov;47(5):656-63. Epub 2009 Jul 24.**IF.: 5,05**

II. Pecze L, Szabó K, Széll M, Jósvay K, Kaszás K, Kúsz E, Letoha T, **Prorok J**, Koncz I, Tóth A, Kemény L, Vizler C, Oláh Z. Human keratinocytes are vanilloid resistant. PLoS One. 2008;3(10):e3419. Epub 2008 Oct 14. **IF.: 0**

c.) Conference presentations related to PhD topic

I. **Prorok J,** Tóth A, Iost N, Kovács PP, Kristóf AA, Tombácz D, Tóth J, Ördög B, Virág L, Papp JG, Varró A, Boldogkői Z.. Herpesvirus-mediated delivery of genetically encoded fluorescent Ca^{2+} sensor to adult canine cardiomyocytes. 32nd Meeting of the European Working Group on Cardiac and Cellular Electrophysiology, Madrid, Spain. 2008

II. **Prorok J.**, Nagy N., Kormos A., Acsai K., Papp Gy., Varró A., Tóth A. 2008 The effect of the NCX inhibitor SEA0400 is intracellular Ca^{2+} level dependent in canine ventricular myocytes. Cardiol. Hungarica, 2008, 38. Suppl.B: B20

III. **Prorok J**, Jost N, Kovács PP. Kristóf A, Tóth A, Ördög B, Boldogkői Z. 2007. Gene transfer into cardiac muscle cells with herpes virus. Cardiologica Hungarica, 37: Suppl A, A24.

ABREVATIONS AND ACRONYSM

$[Ca^{2+}]_i$: intracellular Ca^{2+}

AAVs: adeno associated viruses

AdVs: adenoviruses

AP: action potential

ATP: adenosine-triphosphate

BFP: blue fluorescent protein

CaM: Ca^{2+}-sensitive module: a hybrid of a Ca^{2+} binding domain of calmodulin

CaM: calmodulin

CaMKII: Ca^{2+} -dependent calmodulin-kinase II

cAMP: cyclic adenosine-monophosphate

CAR: coxsackie adenovirus receptor

CFP: cyan fluorescent protein

CICR: Ca^{2+} induced Ca^{2+} release

ECC: excitation contraction coupling

FRET: Fluorescence resonance energy transfer

GECIs: genetically encoded calcium indicators

GFP: green fluorescent protein

I_{CaL}: L-type Ca^{2+} current

KB: Kraft Brühe solution

KH: Krebs-Henseleit solution

M13: myosin light chain kinase peptide

NCX: Na^{+}- Ca^{2+} exchanger

PMCA sarcolemmal Ca2+ ATPase

PRV: pseudorabies virus

RVs: retroviruses

RyR: ryanodine receptor

SERCA: sarcoplasmic reticulum Ca^{2+} ATPase

TnC: troponin C

YFP: yellow fluorescent protein

TABLE OF CONTENTS

1. SUMMARY 6
2. AIMS OF THE STUDY 7
3. INTRODUCTION 8
3.1 Physiology of Ca^{2+} handling in the cardiac myocytes 8
3.2 Altered Ca^{2+} handling in diabetes 10
3.3 Optical measurement of the intracellular calcium concentration 11
4. MATERIALS AND METHODS 15
4.1 Isolation of cardiomyocytes 15
4.2 Induction of experimental type 1 diabetes 17
4.3 Optical measurements 17
4.4 Methods for experiments using GECIs 19
4.5 Chemicals 23
4.6 Data analysis 23
5. RESULTS 24
5.1 Characterization of the NCX inhibiting effect of SEA0400 in canine cardiomyocytes 24
5.2 Evaluation of intracellular Ca^{2+} changes during type 1 diabetes in rabbit myocytes 25
5.3 Herpesvirus-mediated delivery of a genetically encoded fluorescent Ca^{2+} sensor to canine cardiomyocytes. 32
6. DISCUSSION 39
6.1 New challenges in the field of Ca^{2+} signaling research 39
6.2 Effect of SEA0400 on caffeine induced Ca^{2+} transients in canine cardiomyocytes: validation of SEA0400 as a tool to study the Ca^{2+} homeostasis 39
6.3.1 Disturbed Ca^{2+} handling in type 1 diabetes 40
6.3.2 Rest decay experiments 42
6.4 Delivery of troponeon to cultured cardiomyocytes 43
7. CONCLUSIONS AND FUTURE PERSPECTIVES 46
8. REFERENCES 47
9. ACKNOWLEDGEMENTS 51
10. ANNEX 52

1. SUMMARY

The Na^+/Ca^{2+} exchanger (NCX) plays a crucial role in cardiac electrophysiology *via* maintaining ionic distributions between the cytoplasm and the extracellular space, shaping the action potential and modulating the contractile activity of the heart *via* tight regulation of the cytoplasmic [Ca^{2+}]. Since the NCX is the primary transporter to extrude Ca^{2+} from the cells, both the Ca^{2+} content of the cardiomyocytes and magnitude and kinetics of the intracellular Ca^{2+}-transient during action potential are highly dependent on its expression level and functional activity. In spite of its critical function, a relatively selective pharmacological NCX inhibitor (SEA0400) has only recently become available, offering yet unexplored novel possibilities in studying NCX function and malfunction. In our first experimental study we aimed to evaluate the effects of selective, partial NCX inhibition by SEA0400 on Ca^{2+} handling in isolated canine ventricular myocytes.

Since the origin and progression of the pathomechanisms, leading to diabetes-induced cardiomyopathy, are poorly explored, monitoring diabetes induced changes in intracellular Ca^{2+} handling in cardiomyocytes in various functional states may help us to improve our rather limited understanding of the pathophysiology of diabetes-associated heart diseases. This improvement, in turn, may open much needed novel therapeutic avenues for more effective prevention and early treatment of cardiac complications in diabetic patients. In our second study we aimed to investigate in an experimental animal model of Type 1 diabetes the putative perturbations in NCX function, by monitoring shifts in intracellular [Ca^{2+}], following the application of the selective NCX inhibitor SEA0400.

The final part of the present thesis describes a promising methodological work. Virus-mediated gene transfer has recently become an important tool for introduction of recombinant genes into cardiomyocytes, offering the potential to treat both rare and common cardiac disorders. In our third study we have developed a novel, pseudorabies virus vector (PRV)-based technique, which enables the targeted delivery of genetically encoded activity sensors into primary culture of isolated adult canine cardiomyocytes. This system has several advantageous features: 1) the virus enters the cells without destroying the intact physiological properties of the cells for a prolonged period; 2) the virus had no effect on the observed physiological properties. We have shown for the first time, that novel herpesvirus-based vectors can efficiently transduce genes into non-dividing cardiac myocytes, offering an alternative approach for gene transfer in this fastidious experimental object.

2. AIMS OF THE STUDY

Unfortunately, however, there is no single best technique/method with which one can measure local intracellular [Ca^{2+}]. While each method for analyzing Ca^{2+} activity has certain advantages over the others, each also suffers significant drawbacks. Our first goal was to establish a simple, reliable experimental system for the measurement of Ca^{2+} activity, which can provide us with more detailed insights into the Ca^{2+} housekeeping of cardiomyocytes under physiological and pathophysiological conditions. Our second goal was to develop an alternative approach for Ca^{2+} measurement and to test the applicability of the novel technique in the experimental settings of basic cardiac electrophysiology by paying particular attention to the combination of genetically encoded Ca^{2+}-sensors with virus-based gene transfer.

In summary, the primary goals of the experimental work summarized in this thesis were, as follows:

1. **To directly validate the NCX inhibitory effect of SEA0400 on caffeine-induced Ca^{2+} transients in canine cardiac myocytes with undisturbed Ca^{2+} handling.**
2. **To investigate the role of NCX in pathological shifts of Ca^{2+} handling in cardiac myocytes isolated from rabbits with experimental Type 1 diabetes.**
3. **To develop a novel, pseudorabies virus (PRV)-based method for targeted delivery of foreign genes into isolated adult cardiomyocytes in primary culture to facilitate future investigations of subcellular events underlying the patomechanism of the cardiac effects of diabetes**

3. INTRODUCTION

At the cellular level, a wide range of physiological processes, as well as a number of pathomechanisms are also reflected in substantial changes of the intracellular ion milieu. Calcium ion (Ca^{2+}) is a ubiquitous intracellular second messenger, involved in the regulation of a plethora of highly diverse cellular functions such as fertilization, electric signaling, contraction, secretion, memory, gene transcription and programmed cell death.

Because of the importance of Ca^{2+} in biology, numerous techniques/methods for analyzing the mechanisms of cellular and/or subcellular Ca^{2+} activity have been established. Since the first attempt to monitor intracellular Ca^{2+} dynamics by Tsien et al. [1] fluorescence based Ca^{2+} signal research has undergone a tremendous development, and is still being improved. In the first part of my thesis I summarize the theoretical background, as well, as the substantial limitations of the conventional Ca^{2+}-sensitive dye-based fluorescence technique widely used to (semi)quantitatively evaluate shifts in intracellular Ca^{2+} levels and distribution and also discuss the principles of promising new enhancements of the classical methodology.

3.1 *Physiology of Ca^{2+} handling in the cardiac myocytes*

From the ions involved in the intricate workings of the heart, calcium is considered perhaps to be the most important. Ca^{2+} is crucial to the complex process called excitation–contraction coupling that enables the heart to contract and relax. In order to understand the physiological regulation of the mechanical activity of the heart, it is important to describe in details, how calcium is transported between the various intracellular compartments of the cardiomyocyte during activation and termination of the contraction

During the cardiac action potential (AP), Ca^{2+} enters the cell *via* depolarization-activated (primarily L-type) Ca^{2+} channels as an inward current (I_{Ca}), which substantially contributes to shaping the plateau phase of the AP.

The primary Ca^{2+} entry triggers a secondary Ca^{2+} release from the sarcoplasmic reticulum (SR). Each junction between the sarcolemma (T-tubule and surface) and SR, where 10–25 L-type Ca^{2+} channels and 100–200 ryanodine receptors (RyRs) are clustered, constitutes a local Ca^{2+} signaling complex. When an L-type Ca channel opens, local $[Ca^{2+}]_i$ rises and Ca^{2+} is released from the sarcoplasmic reticulum (SR) via the RyRs during the course of a process called Ca^{2+}-induced Ca^{2+} release [2]. In this phase of the action potential, the Na^+/Ca^{2+} exchanger can also contribute to the Ca^{2+} influx (reverse mode operation) since the membrane potential is positive and the intracellular Ca^{2+} level is low. However, when -

due to the Ca^{2+} induced release of Ca^{2+} from the sarcoplasmic reticulum - the intracellular Ca^{2+} level increases at the beginning of the intracellular "Ca^{2+} transient", the Na^{+}/Ca^{2+} exchanger turns into forward mode operation, thereby contributing to the extrusion of Ca^{2+} from the cell (Fig. 1) [3, 4]

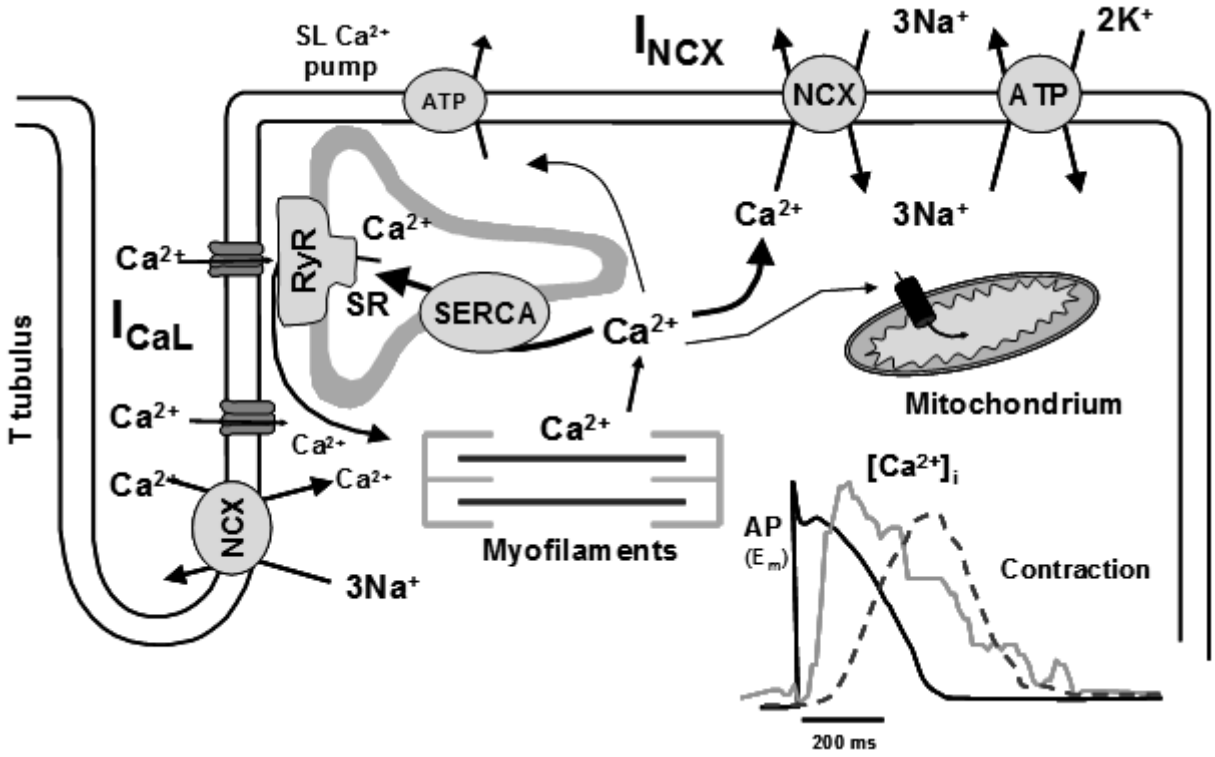

Figure 1 Major Ca^{2+} transport pathways in ventricular cardiomyocytes. The insert shows the time course of an action potential, Ca^{2+} transient and contraction measured in a rabbit ventricular myocyte at 37°C. Abbreviations: SR: sarcoplasmic reticulum; NCX: Na^{+}/Ca^{2+} exchanger; ATP: Plasma-membrane Ca^{2+}-ATPase & Na^{+}/K^{+} -ATPase; SERCA: SR Ca^{2+}-ATPase (Bers DM, 2002)

The combination of Ca^{2+} influx and release significantly raises the free intracellular Ca^{2+} concentration ($[Ca^{2+}]_i$), allowing Ca^{2+} to bind to the myofilament protein troponin C, which in turn switches the contractile machinery on. Although Ca^{2+} is the switch that activates the myofilaments, the contraction is graded and depends not only on $[Ca^{2+}]_i$ but also on several other factors. The amount of total cytosolic $[Ca^{2+}]$ ($[Ca^{2+}]=[Ca^{2+}]_i$ plus bound Ca^{2+}) that must be supplied to and removed from the cytosol during each cardiac beat. For relaxation to occur $[Ca^{2+}]_i$ must decline, allowing Ca^{2+} to dissociate from troponin. This requires Ca^{2+} transport out of the cytosol by four pathways as follows: 70-90 % of the cytoplasmic Ca^{2+} is resequestrated into the sarcoplasmic reticulum by the sarcoplasmic reticulum Ca^{2+} ATPase (SERCA2), 7-30 % is extruded from the cell by the Na^{+}/ Ca^{2+} exchanger, and only a small amount of Ca^{2+} is extruded by the slow Ca^{2+} transport systems, such as the sarcolemmal Ca^{2+} ATPase (PMCA) and the mitochondrial Ca^{2+} transport [5]. For steady contractile activity of

the heart the amount of Ca^{2+} extruded during relaxation and the amount of Ca^{2+} entry during each beat must be the same, otherwise the cell would either gain or lose Ca^{2+}. Indeed, complementary measurements of Ca^{2+} influx and SR Ca^{2+} release during a twitch confirm this expectation. This provides a quantitative framework for dynamic Ca^{2+} fluxes in ventricular myocytes. The ability of the NCX to carry both inward and outward I_{NCX} during the same AP and the role of NCX in Ca^{2+} extrusion, generation of pacemaker activity and cardiac arrhythmias arrhythmias make crucial the detailed understanding the role of this transporter in Ca^{2+} handling in normal as well as in pathological conditions.

3.2 Altered Ca^{2+} handling in diabetes

Ca^{2+} handling is directly or indirectly involved in all major types of cardiac diseases, such as heart failure or cardiac arrhythmias. Diabetes is becoming an increasing health problem worldwide. Although diabetes is associated with a variety of pathological processes, including renal failure and neuropathies, heart disease is the leading cause of mortality among diabetic patients [6]. Although coronary artery disease is considered to be the major complication associated with diabetes, diabetic cardiomyopathy - characterized by decreased contractile performance - is observed even in the absence of notable coronary artery disease [6]. Although the diabetic state affects a number of aspects of normal cardiac myocyte physiology, including alterations in intracellular signaling pathways and energy substrate metabolism, numerous studies have suggested that SR dysfunction, leading to alterations in calcium handling is, indeed, responsible for the decreased contractile performance [7, 8]. This decrease has been demonstrated *in vivo* and *in vitro*, in isolated heart and cardiac myocyte preparations. Diabetic cardiomyopathy manifests itself as a decrease in absolute force production, as well as declined rate of force development, indicating that multiple aspects of Ca^{2+} handling may be involved [9].

Despite the recent advances in this field, our understanding of the initiation and progress of diabetic cardiomyopathy is highly limited. In my thesis I will present the first results of our group in this field, in which study we investigated the possible role of the NCX in the pathological shift in Ca^{2+} handling in type I diabetes. For this purpose, we used a recently developed NCX inhibitor SEA0400. In the present thesis we also discuss the validation of SEA0400 as an appropriate NCX inhibitor in intact cardiac myocytes.

3.3 Optical measurement of the intracellular calcium concentration

It is known that Ca^{2+} as a second messenger regulates a wide range of physiological cellular mechanisms. However, it can also trigger pathomechanisms, such as cell injury and death, neurodegeneration, skeletal muscle defects, heart disease and skin disorders. A number of techniques have been developed to quantitate intracellular Ca^{2+} levels. The majority of these techniques utilize fluorescent Ca^{2+} indicators. Essentially, these indicators show an increase in magnitude or a shift in their fluorescence spectrum upon binding to Ca^{2+}. There are two major classes of Ca^{2+} indicator dyes: chemically engineered fluorescent dies and genetically encoded fluorescent proteins. The use of these fluorescent Ca^{2+} indicators has been a highly successful approach to study the role of Ca^{2+} in specific intracellular processes and rapidly advanced our understanding of the underlying mechanisms of Ca^{2+} signaling as well as our appreciation for the ubiquitous role of Ca^{2+} in cellular activities.

3.3.1 Chemically engineered fluorescent indicators

The most widely used fluorescent Ca^{2+} indicators are chemical probes, because, in general, either the spectral or the intensity change in their fluorescence is relatively large for a given change in $[Ca^{2+}]$ compared with other types of Ca^{2+} indicators. Most of the classical members of this group were produced by Tsien and colleagues [1, 10, 11]. One way to classify these probes into two subgroups is whether they are used as non-ratiometric (single wavelength) or ratiometric indicators. Fluo-3, fluo-4, the calcium green class, and rhod-2 are non-ratiometric, whereas indo-1 and fura-2 are ratiometric dyes. Both subgroups require specific equipment, such as excitation sources, interference filters, and detection techniques, according to their spectral properties and both subclasses have advantages and limitations as well. Fluo-3 and Fluo-4 are probably the most suitable Ca^{2+} indicators, for their simple use in a wide variety of isolated cell types. Fluo-4 is a brighter, more photostable derivative of Fluo-3. Its Ca^{2+} affinity is slightly lower (Kd 345 nM) and its absorption maximum is shifted by 12 nm compared to Fluo-3, making it more suitable for 488 nm excitation by an argon laser [12]. Because of the lower Kd, fluo-4 can be used at a lower dye concentrations and thus, it is less phototoxic. Fluo-4 has very low background absorbance and the lower dye concentrations require shorter incubation times [13]. These properties qualify fluo-4 for optimal intracellular free Ca^{2+} measurement in beating myocytes.

3.3.2 Genetically Encoded Calcium Indicators (GECIs)

Green fluorescent protein (GFP) is a photosensitive protein originally isolated from the jellyfish *Aequorea victoria*. GFP absorbs the blue luminescent emission of aequorin and gives off green fluorescence in A. victoria [14]. The cloning of GFP gene made possible to fuse its DNA to that of cellular constituents, wich has led to the use of GFP as markers of gene expression and protein localization in living organisms [15, 16]. The use of GFP and its derivatives have become one of the most popular and exciting new techniques in cell biology. Some groups have successfully constructed GFP based Ca^{2+} indicators (Fig 2.). Miyawaki and colleagues [17] have expressed GFP-based Ca^{2+} indicators (called "chameleons") in the cytosol and endoplasmic reticulum of intact HeLa cells. Cameleons consist of four major functional units: two GFP variants emitting fluorescence at different wavelengths, the Ca^{2+}-sensitive protein calmodulin and M13, a 26 amino acid long residue of calmodulin-binding peptide of myosin light-chain kinase. The hybrid protein (calmodulin-M13 complex) bridges the two GFP mutants. When Ca^{2+} binds to the calmodulin in this complex, the hybrid protein changes its conformation, which results in the decrease in the distance between the two GFP mutants and an increase in fluorescence resonance energy transfer (FRET). This first version of Cameleon has been progressively modified in several ways including a decrease in pH sensitivity of the photon acceptor in the yellow cameleons [18, 19].

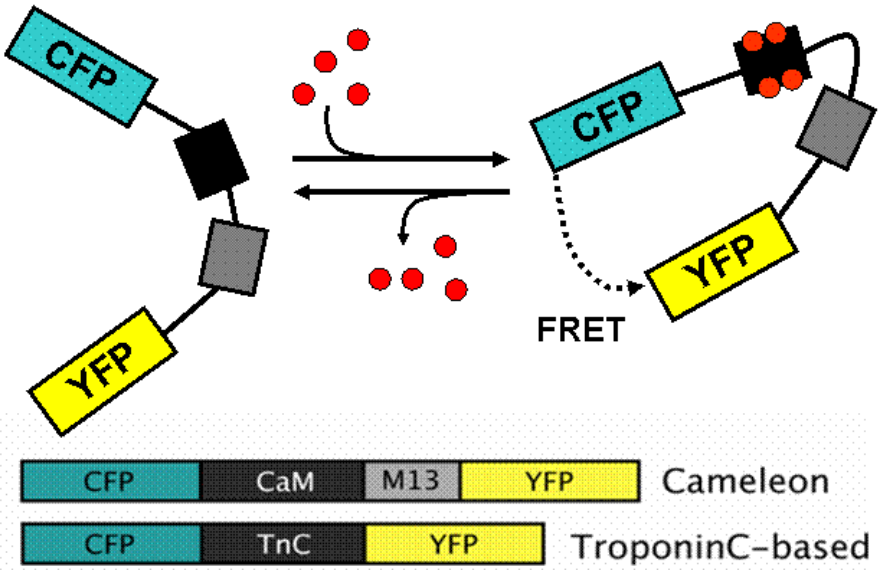

Figure 2. Working schema of GECIs. GECIs consist of two GFP variants (CFP and YFP) of which spectra allow FRET between them when all other required conditions are met and a Ca^{2+}-sensitive module: a hybrid of a Ca^{2+} binding domain of calmodulin and the M13 myosin light chain kinase peptide or troponin C in case of Cameleon and Troponeon, respectively. Binding of Ca^{2+} to the Ca^{2+}-sensitive module results in conformation changes which in turn facilitates FRET between CFP and YFP. Lower paner: Schematic map of the Cameleon and Troponeon GECIs.

Roger Tsien and coworkers demonstrated two improved combinations of donor and acceptor GFP mutant pairs, blue fluorescent protein (BFP)/GFP and cyan fluorescent protein (CFP)/yellow fluorescent protein (YFP). Their excitation wavelength and emission ratio are 380–510/445 and 440–535/480 nm, respectively [19].

Heim and Griesbeck [20] developed novel types of calcium probes called troponeons. Troponeons are based on troponin C variants from skeletal and cardiac muscle, and mutants of the green fluorescent protein (CFP and citrine). Troponeon has ratio changes up to 140%, Kd values ranging from 470 nM to 29 μM, and improved subcellular targeting properties. The authors clearly demonstrate their usefulness of troponeons for dynamic Ca^{2+} imaging within live cells.

3.3.3 Benefits and pitfalls: chemically versus genetically encoded Ca^{2+} indicators

A major advantage of chemical indicators over genetically encoded fluorescent proteins is the broad range of dyes of various Ca^{2+} affinities that are commercially available for the user and the relative easy of use of the these dyes for experiments. Chemical Ca^{2+} indicators are easy to introduce into cells, cell-loading protocols for chemical Ca^{2+} indicators have been well-established [21]. A major disadvantage is that the intracellular localization of these Ca^{2+} indicators cannot be easily controlled or specifically targeted to a particular organelle. In addition, chemical indicators tend to compartmentalize and are eventually extruded from the cell during long recording experiments [22]. A relatively simple, yet successful strategy to combat the compartmentalization problem has been to generate indicators with a large dextran tag [23]. This strategy permits extended periods of Ca^{2+} level recordings up to days at a time. However, a limitation of dextran tagged dyes is that they are more difficult to load and generally need to be directly injected into cells.

GECIs are not expressed endogenously, their genetic material needs to be introduced experimentally. GECIs can be stably expressed by genetic modifications of the cell line or the animal that is being studied, or they can be transiently expressed by one of the physicochemical or virus-based gene transfer techniques. Therefore, the use of GECIs relies on sophisticated molecular biological infrastructure in most of the cases. On the other hand, among the several others, the most important advantage GECIs offer is the possibility to target specific cellular compartments or specific subcellular loci by creating fusion proteins of a GECI and an endogenously expressed protein or by using special targeting sequences, the so-called signal peptides [13]**.** The latter two techniques may allow us to study Ca^{2+} fluctuations at specific subcellular locations.

3.3.4 Gene transfer techniques: advantages and limitations

Viruses had millions of years to evolve the ability to efficiently infect their host cells. During infection, the viruses deliver their own genetic material into the host cell, which ability can be employed by utilizing viruses as vectors for delivering exogenous genes to a broad range of cell types. Virus-mediated gene transfer methods have become powerful and widely used experimental tools in biological research. In the case of adult cardiomyocytes the efficiency of most of the gene transfer techniques that work well in other systems is highly limited because cardiac cells do not divide, have a relatively short lifetime in culture and are highly sensitive to toxic effects. Gene transfer methods in general and in cardiovascular research as well can be divided into two groups: physicochemical (or non-viral) and viral vector-based systems. Non-viral methods involve cationic liposome/plasmid DNA complexes, incubation with naked DNA, and calcium phosphate precipitation [24, 25]. Non-viral techniques suffer from severe limitations such as very low transfection efficiency especially in *in vivo* applications, cytotoxicity and short-term expression of transduced genes due to intracellular degradation of foreign DNA. The above limitations urged the application of more efficient virus vector-based approaches for gene delivery to the cardiovascular system. The following viral systems have been applied in molecular cardiology: adenoviruses (AdVs), adeno-associated viruses (AAVs), retroviruses (RV) like lentivirus (HIV-1) and herpes simplex virus (HSV-1)-derived vectors [24, 25]. Currently, AdVs and AAVs are the most frequently used tools for delivering genes into the cells of the cardiovascular system, both *in vivo* and *in vitro* [26, 27]. While AdV–based vectors allow relatively highly efficient delivery of transgenes to cardiac cells, this system provides only transient expression of transferred genes since the virus does not integrate into the host genome [28]. The application of AdVs have further limitations including strong immune responses by the host organism, limited payload size and during propagation may have moderately difficult quality control. An additional problem with AdV systems is related to the infection efficiency. The coxsackie adenovirus receptor (CAR) is a key determinant for the attachment and cellular uptake of AdVs [29]. However, CAR expression is maximal in neonates and is reduced rapidly after birth in several organs such as heart, muscle and brain resulting in lower penetration rate of adenovirus vectors [30]. Recombinant AAV vectors are able to effectively transduce foreign genes to a variety of cell types including both dividing and post-mitotic cells in both *in vitro* and *in vivo* experimental systems [31]. The AAV-based systems have a number of favourable attributes, such as minimal immunogenicity, lack of parental agent pathogenicity and vector-related cytotoxicity, and the capacity for stable long-term transgene expression. The main

disadvantages of AVV vector–based approaches include the difficulty of producing high-titer virus stocks of consistent purity and bioactivity, and the limited packaging capacity of a maximum 4.8 kb insert-size [32]. Lentivirus-based gene transfer has been reported in a wide variety of cell types, including cardiomyocytes [33]. Current lentiviral vectors are capable of transducing mitotically quiescent cells, particularly within the cardiovascular system. The strengths of this system include the ability of long-term stable transgene expression, an increased packaging capacity compared with AAV, and the other commonly used integrating vector [34]. The disadvantages of lentivirus-based gene delivery systems are the relative low level of transgene expression and the limited transgene carrying capacity of the virus.

Pseudorabies virus (PRV), a causative agent of Aujeszky's disease of swine, is an alpha-herpesvirus belonging to family of Herpesviridae. Several previous reports have been successful in construction of PRVs for delivering foreign genes to neurons [35]. PRV is an especially important tool for labelling neuronal circuits [36], which was combined with delivery of activity markers to labelled neurons [37]. Application of PRV-based gene transfer vectors in the cardiovascular research field has not yet been reported.

4. MATERIALS AND METHODS

4.1 Isolation of cardiomyocytes

All experiments were conducted in compliance with the Guide for the Care and Use of Laboratory Animals. The protocols were approved by the review board of the Committee on Animal Research of the University of Szeged, Szeged, Hungary.

New Zealand rabbits weighing 1.5 - 2.0 kg were used. Each animal was anaesthetized by intravenous infusion of 30 mg kg^{-1} pentobarbital and sacrificed by cervical dislocation after an intravenous injection of 400 IU kg^{-1} heparin. Rabbit ventricular myocytes were produced by enzymatically dissociation. The chest was opened, the heart quickly removed and placed into cold (4°C) Krebs-Henseleit (KH) solution with the following composition (mM): NaCl 135, KCl 4.7, KH2PO4 1.2, $MgSO_4$ 1.2, HEPES 10, $NaHCO_3$ 4.4, Glucose 10, $CaCl_2$ 1.8. The pH of this solution was 7.4 when saturated with a mixture of 95% O_2 and 5% CO_2. The heart was then mounted on a modified Langendorff column (Fig. 3) and perfused with oxygenated perfusate of the same composition warmed to 37°C. Perfusion was continued with Ca^{2+}-free Krebs-Henseleit solution for further 5 min, then the perfusate was completed with collagenase (0.05 %, type I), hyaluronidase (0.05 %) and $CaCl_2$ (200 μM) and the heart was perfused for additional 15 min. Finally the left ventricular myocardium was minced and

gently agitated. The cells freshly released from the tissue were stored in storage solution at room temperature before use.

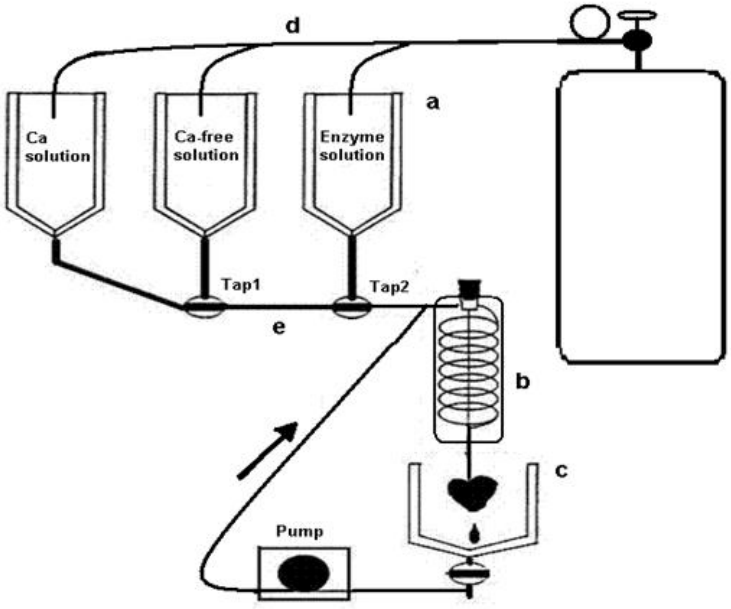

Figure 3. Schematic illustration of the Langendorff apparatus used to isolate single cardiac myocytes at 37°C from beating heart. The apparatus consists of: a) Temperature controlled (37°C) water-jacketed solution reservoirs (300 ml). b) Glass-coil heat exchanger with heart cannula and bubble trap; c) Water-jacketed reservoir to warm the heart and collect recirculating solution; d) Gas bubblers e) Three-way taps for rapid switching between solutions.

The storage solution contained in mM: KOH 89, L-glutamic acid 70, taurine 15, KCl 30, KH_2PO_4 10, HEPES 10, $MgCl_2$ 0.5, glucose 11, EGTA 0.5, and pH was set to 7.3 with KOH. The cells were rod shaped and showed clear striation when the external calcium was restored. Using the apparatus shown in Figure 3, rabbit hearts were perfused retrogradely through the aorta, and thus through the coronary arteries, which supply the muscle of the ventricles. The same apparatus, with modified solution flow-rates and cannulae, was used for canine left ventricle isolations.

Canine ventricular myocytes were enzymatically dissociated as follows. A portion of the left ventricular wall containing an arterial branch large enough to cannulate was perfused in a modified Langendorff apparatus (Fig. 3) with solutions in the following sequence: 1) normal Tyrode's solution (10 min), 2) Ca^{2+}-free Tyrode solution (10 min), and 3) Ca^{2+}-free Tyrode solution containing collagenase (type I, 0.66 mg/ml) and bovine serum albumin (fraction V, fatty acid free, 2 mg/ml) (15 min). Protease (type XIV, 0.12 mg/ml) was added to the final perfusate while and another 15 - 30 min of digestion was allowed. Cells were stored in Kraft Brühe (KB) solution. The composition of solutions were (in mM): a) normal Tyrode's

solution - NaCl 135, KCl 4.7, $KH2PO_4$ 1.2, $MgSO_4$ 1.2, HEPES 10, $NaHCO_3$ 4.4, glucose 10, and $CaCl_2$ 1.0 (pH 7.2 adjusted with NaOH); b) Ca^{2+}-free Tyrode solution - NaCl 135, KCl 4.7, KH_2PO_4 1.2, $MgSO_4$ 1.2, HEPES 10, $NaHCO_3$ 4.4, Glucose 10, and taurine 20 (pH 7.2 adjusted with NaOH); c) KB solution - KOH 90, L-glutamic acid 70, taurine 15, KCl 30, KH_2PO_4 10, $MgCl_2$ 0.5, HEPES 10, glucose 11, and EGTA 0.5 (pH 7.3 adjusted with KOH). All chemicals used in this method were purchased from Sigma Chemical Co.

4.2 Induction of experimental type 1 diabetes

This protocol for induction of diabetes was based on established procedures described earlier Lengyel et al. [38]. Briefly, male New Zealand white rabbits (n = 19), weighing 1.5–2.0 kg, were used in this experiment. Diabetes mellitus was induced in 10 rabbits by infusion of a single intravenous dose of alloxan (145 mg kg-1) (alloxan monohydrate, Sigma, St Louis, MO, USA) into the ear vein under pentobarbital anaesthesia (26–30 mg kg^{-1} i.v., Nembutal; CEVA, Paris, France), after fasting overnight. Blood glucose was measured twice weekly from blood samples obtained from the ear vein. Untreated animals were used as controls. Body weight and plasma glucose levels were determined in each animal at the beginning as well as at the end of the experiment (just prior to the electrophysiological analysis). We opted for this 3-week model based on previous studies performed in streptozotocine-induced rat/mouse models, where the electrophysiological remodelling effects were investigated after 2–4 weeks of diabetic period [39, 40] After 3 weeks diabetic rabbits were used for myocyte isolation and intracellular calcium measurements.

4.3 Optical measurements

Simultaneous recording of caffeine induced and steady-state $[Ca^{2+}]_i$ transients and cell shortening in field stimulated cardiomyocytes

Freshly isolated myocytes were loaded by incubation for 20 min with the acetoxymethyl ester (AM) form of a single wavelength calcium-sensitive fluorescent dye (Fluo-4, Molecular Probes Inc. 2 μM from a stock of 1 mM in DMSO +20% pluronic acid) at room temperature. Loaded myocytes were mounted in a low volume imaging chamber (RC47FSLP, Warner Instruments,). and placed on the stage of an inverted fluorescent microscope (IX71, Olympus, Japan) and the cells were superfused with normal Tyrode solution at 37ºC (1ml/min).

Caffeine was originally isolated from coffee such as white crystalline xanthine alkaloid which is a psychoactive stimulant in the central nervous system. Among its numerous effects

it also induces Ca^{2+} transient in heart muscle cell through activating RyRs. $[Ca^{2+}]_i$ transients were induced by applying 5 mL caffeine (10 mM)-containing Tyrode solution for 6 s at a flow rate of 50 mL/min directly onto the cell surface from a micropipette. These micropipettes, having typical tip diameter of 100 μm, were positioned by a manipulator to ~100 μm distance from the cell. The control caffeine flush was repeated after 2 min, then 1 μM SEA0400 was superfused for 5 min, and the caffeine flushes were applied again. The 2 min period of time spent between the consecutive flushes was sufficient for the cells to recover from the caffeine transient, i.e. the two subsequent challenges yielded close to identical responses, otherwise data were discarded. The two control and two SEA0400 curves were corrected against dark current, non-specific background, and bleaching artefact, averaged, and normalized so as to have identical amplitudes. When studying the effect of Ni^{2+}, the cells were exposed to 10 mM $NiCl_2$-containing Tyrode for 15s prior to the beginning of the caffeine pulse and Ni^{2+} concentrations were maintained throughout the caffeine exposure.

For steady-state $[Ca^{2+}]_i$ measurements myocytes were stimulated at a constant frequency of 1 Hz through a pair of platinum electrodes by an electronic stimulator (Experimetria Ltd, Hungary). The dye was excited at 480 nm, fluorescence emission was recorded at 535 nm (Chroma, USA). Optical signals were recorded by a photon counting photomultiplier module (H7828, Hamamatsu, Japan) and sampled at 1 kHz. Measurements were performed and data were analyzed using the Isosys software (Experimetria, Hungary). Cell shortening from both ends was determined by a video edge detection system (VED-105, Crescent Electronics, Sandy, Utah, USA) (Fig 4.). All data are expressed as mean ± SEM.

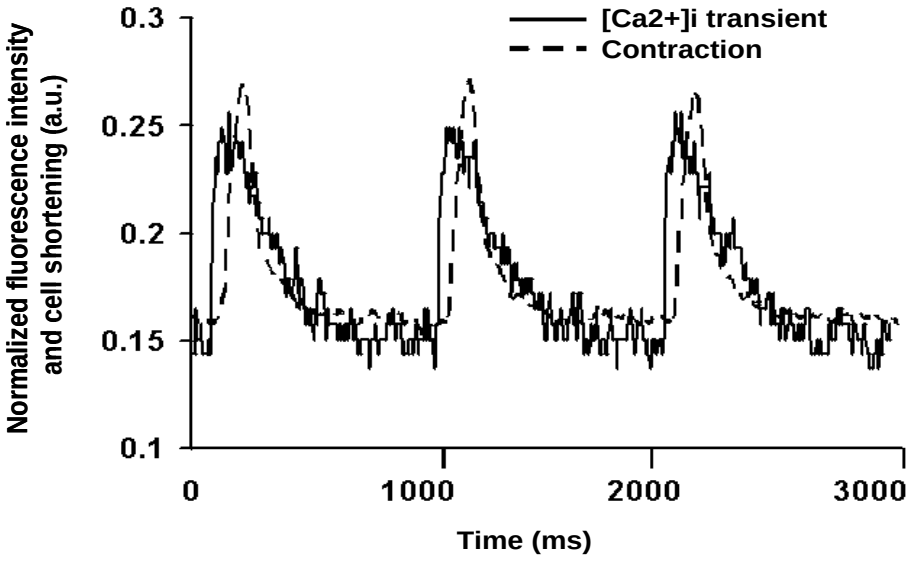

Figure 4. Representative recordings of the intracellular Ca^{2+} transient and cell shortening. These parameters are detected in parallel by a photon counting system and a video edge detector.

4.4 Methods for experiments using GECIs

Reporter genes

A troponeon variant (Tn-15), [20] was used as a GECI. The troponeon gene was placed under the control of the major immediate early promoter of human cytomegalovirus (pCMV), which provided a high level of gene expression. The marker gene expression cassette also contained simian virus 40 (SV40)-derived sequences including polyadenylation signal and transcription termination sequences. In addition, a lacZ gene equipped with the above regulatory sequences was also used as a reporter gene for the identification of mutant viruses.

Construction of targeting vectors

In our molecular cloning system, we use so-called targeting plasmids that combine with the parental virus genome by homologous recombination. A typical targeting plasmid contains a gene expression cassette of the gene that is to be introduced into the virus genome and subcloned viral DNA sequences flanking the expression cassette, which serve as homologous DNA regions for the recombination. The homologous recombination that occurs between the targeting plasmid and the virus genome results in a modified virus genome that carries the expression cassette. To adapt for applicability as virus vector we deleted the two ribonucleotide reductase (rr) and the early protein (ep0) genes from the virus genome by homolog recombination. The rr1 and rr2 genes are in charge for production of raw material of viral DNA. The recombinant virus is not able to productively infect postmitotic cells without rr genes, while ep0 gene is responsible for virus reactivation from latency. Troponeon gene (csTnC-L15) was inserted to antisense internal and external repeat (IR, TR) region in two copies. The DNA sequences used for mutagenesis and as insertion sites for reporter genes are listed in Fig. 5.

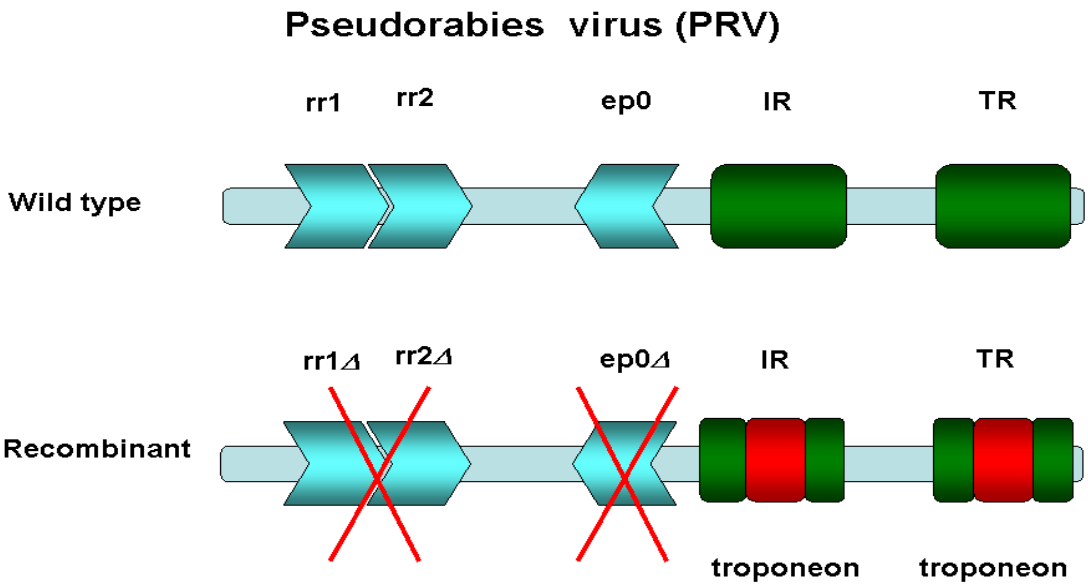

Figure 5. This panel shows the schematic illustration of wild type and recombinant herpes virus genom. Abbreviations: rr1: ribonucleotide reductase 1; rr2: ribonucleotide reductase 2; ep0: early protein 0; IR: inner repeat; TR: external repeat

Culture and infection of myocytes

The protocol for cell isolation was based on established procedures described earlier in chapter "4.1 Isolation of cardiomyocytes".

The entire culture procedure was performed in a class II flow hood. The freshly isolated myocytes were centrifuged five times for 1 min at 50 g in sterile 10% PBS. The supernatant was replaced first by 500 µM then by 1 mM Ca^{2+} containing PBS solution. The mild centrifugation steps removed the majority of bacterial cells, most non-myocytes and non-functioning myocytes. Precipitated cells were resuspended in culture medium and plated on laminin coated (1 µg/cm2) sterile cover glass at densities of up to 10^3 rod-shaped cells cm^{-2}. Cells were left 4 hours to attach to the plate and after this time period non-attached cells were removed. Following the first medium change, subsequent medium changes were carried out every day. Culture medium consisted of serum-free medium 199 (M199) supplemented with 25 mM $NaHCO_3$, 5 mM ceratine, 2 mM L-carnitine, 5 mM taurine, 100 units/ml insulin (CCTI supplemented medium) and 50µg/ml gentamycin. All chemicals used in this procedure were purchased from Sigma. Cells were maintained at 37°C under sterile conditions in an incubator ventilated with 5% CO_2 and 95% air. After 4 hours, plate attached cells were infected. Freshly isolated canine cardiomyocytes were first washed with PBS, followed by low-speed centrifugation and resuspension in culture medium. Subsequently, after 4-hour

incubation at 37 °C in a CO_2 incubator, cells were infected with various titers of recombinant viruses for 12 hours then washed and the culture medium was changed. Infected cells were used for analysis at various time points.

Evaluation of infection efficacy and morphological changes in cultured cells

Cell shape and morphology are closely linked with some aspects of cell function such as excitation–contraction coupling. Therefore, monitoring these properties may give indications of physiological changes that are occurring. Morphological changes of cells were observed by light microscopy on a daily basis parallel with physiological measurements. Troponeon-positive cells were examined by fluorescence microscopy from one to three days following isolation at standard titer of viruses. Infection efficacy was determined separately for infected cells by manual cell counting using a fluorescent microscope (Olympus IX-71).

Evaluation of the electrophysiological state of the cells by I_{to} analysis

I_{to} currents were measured using the whole-cell configuration of the patch-clamp technique. Measurements were performed daily starting with day 0, when only freshly isolated non-infected myocytes were investigated. In the following days control and infected cells were studied separately by placing cover glasses with the attached cells in the recording chamber mounted on the stage of an inverted microscope equipped with epifluorescence assembly (Olympus IX50, Tokyo, Japan). Only rod-shaped cells with clear cross striations and relatively strong GFP signal were used. HEPES-buffered Tyrode's solution containing (in mM): NaCl 144, NaH_2PO_4 0.33, KCl 4.0, $CaCl_2$ 1.8, $MgCl_2$ 0.53, glucose 5.5 and HEPES 5.0 at pH of 7.4 (by NaOH) served as normal superfusate. Cell capacitance (199.3±13.7 pF, n=69) was determined by applying a 10 mV hyperpolarizing pulse from a holding potential of -10 mV. Cell capacity was calculated as the integral of the capacitive transient divided by the amplitude of the voltage step. Patch-clamp micropipettes were fabricated from borosilicate glass capillaries (Clark, Reading, UK) using a P-97 Flaming/Brown micropipette puller (Sutter Co, Novato, CA, USA). These electrodes had resistances between 1.5 and 2.5 Mohms when filled with pipette solution containing (in mM): K-aspartate 100, KCl 45, K_2ATP 3, $MgCl_2$ 1, EGTA 10 and HEPES 5. The pH of this solution was adjusted to 7.2 by KOH. Membrane currents were recorded with Axopatch-200B patch-clamp amplifiers (Axon Instruments, Foster City, CA, USA). After establishing a high (1-10 GOhm) resistance seal by gentle suction, the cell membrane beneath the tip of the electrode was disrupted by suction or by application of 1.5 V electrical pulses for 1 - 5 ms. The series resistance was typically 4 – 8

MOhm before compensation (50 - 80%, depending on the voltage protocols). Experiments where the series resistance was high, or substantially increased during measurement, were discarded. Membrane currents were digitized using a 333 kHz analogue-to-digital converter (Digidata 1200, Axon Instruments) under software control. Analyses were performed using pClamp 8.0 (Axon Instruments) software after low-pass filtering at 1 kHz. All patch-clamp data were collected at 37 °C.

Evaluation of cell function by monitoring $[Ca^{2+}]_i$ transient and cell shortening.in field stimulated primary cell culture

24-72 hours following culturing or viral infection cardiomyocytes were loaded with the acetoxymethyl ester (AM) from a single wavelength calcium-sensitive fluorescent dye (Fluo-4, Molecular Probes Inc. 2μM) at room temperature. The technique for calcium transient detection was based on established procedures described earlier in chapter "Recording of $[Ca^{2+}]_i$ transients and cell shortening in field stimulated myocytes"

Evaluation of the functionality of the transduced GECI

To test full functionality of the transferred troponeon gene, calcium transients were monitored using a dual channel photon counting system in cardiomyocytes expressing troponeon. The troponeon was excited at 480 nm, fluorescence emission was recorded at 535 and 485nm (Chroma, USA). The cells were superfused with normal Tyrode solution at 37ºC (1ml/min). Myocytes were stimulated at a constant frequency of 1 Hz. The cells were superfused with normal Tyrode solution at 37ºC (1ml/min). Myocytes were stimulated at a constant frequency of 1 Hz through a pair of platinum electrodes by an electronic stimulator. Optical signals were recorded by two photon counting photomultiplier module (H7828, Hamamatsu, Japan), and sampled at 1 kHz. Changes in $[Ca^{2+}]_i$ levels were characterized by the ratio of emitted fluorescence intensities obtained at 485 and 535 nm wavelengths, ($F_{CITRINE}$ 535 / F_{CFP} 485) following correction for non-specific background fluorescence.

4.5 Chemicals

All chemicals were purchased from Sigma-Aldrich (St. Louis, MO, USA), except SEA0400 and Fluo-4 AM. Calium sensitive fluorescent dye Fluo-4 AM was purchased from Molecular Probes Inc. (Eugene, Oregon, USA). SEA0400 was synthesized based on the description of Aibe et al. (2000) at the Department of Pharmaceutical Chemistry (University of Szeged, Hungary). SEA0400 was dissolved in dimethyl sulfoxide (DMSO) and its final concentrations were 0.3 or 1 μM when diluted in Tyrode solution.

4.6 Data analysis

The fluorescent recordings were corrected for background fluorescence and the change of fluorescence intensity by bleaching in the case of troponeon expressing cells.

All results and optical measurements were compared using Student's t-tests for paired and unpaired data and expressed as mean ± SEM values. Statistical significance of differences obtained between control and virus infected preparations was evaluated with Student’s t-test for paired or unpaired data, as relevant. Differences were considered significant when $p<0.05$.

5. RESULTS

5.1 Characterization of the NCX inhibiting effect of SEA0400 in canine cardiomyocytes

Previous studies demonstrated that SEA0400 may have different efficacy in inhibiting the NCX, depending on the intracellular ionic composition [41]. These results may question the use of SEA0400 as a research tool in the Ca^{2+} handling research. Therefore in our first experiments we characterized the NCX inhibiting effect of SEA0400 in a setting, where long lasting, high $[Ca^{2+}]_i$ level was achieved by the application of 10 mM caffeine. Under these conditions Ca^{2+} dependent NCX inhibiting effect of SEA0400 can be assumed to be maximal, consequently, in the experiments on the diabetic rabbit heart cells the actual degree of NCX block was presumably at least as high as in the caffeine experiments. Since the relaxation kinetics of a $[Ca^{2+}]_i$ transient reflects the kinetic properties of Ca^{2+} elimination from the cytosol, NCX inhibition should be reflected in an elongation of the decay of $[Ca^{2+}]_i$ transients. Therefore, the effect of 1 μM SEA0400 was studied on $[Ca^{2+}]_i$ transients evoked by superfusion with 10 mM caffeine for 6 s.

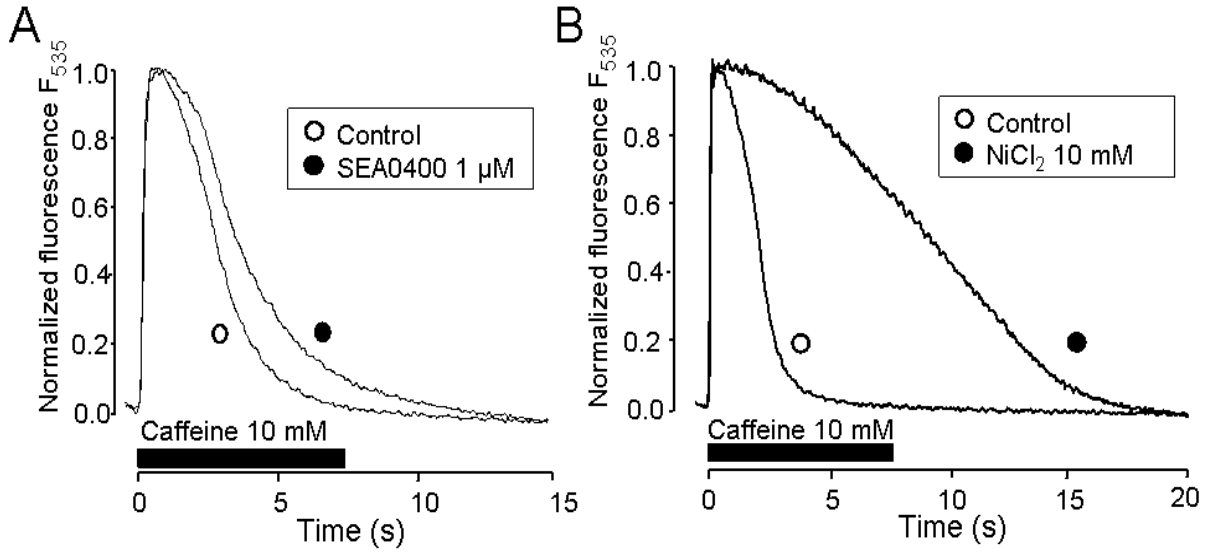

Figure 6 Representative superimposed records showing the effect of 1 mM SEA0400 **(A)** and 10 mM $NiCl_2$ (B) on the time course of the $[Ca^{2+}]_i$ transients elicited by superfusion of 10mM caffeine for 6 s. Before the application of caffeine, the myocytes were continuously paced at a frequency of 1 Hz.

In order to compare the time course of decay, the transients were normalized to identical amplitudes and superimposed (Fig. 6).The decay time constant, determined using mono-exponential fit, was significantly increased by 1 μM SEA0400 from 1.03±0.05 to 1.32±0.06 s ($P< 0.05$, $n = 10$), whereas the respective time-matched control values (i.e. when SEA0400 was omitted from the solution) were 0.96±0.05 and 0.95±0.04 s (n=8). These results directly

prove that under the given conditions, SEA0400 is capable to partially inhibit NCX. The NCX-blocking potency of SEA0400 can be qualitatively evaluated by comparing with that of 10 mM $NiCl_2$, which is known to fully block the exchanger. As in the presence of $NiCl_2$ the decaying limb could not be fitted exponentially, the time of half-relaxation was determined: it was increased by $NiCl_2$ from 1.3±0.1 to 10.1±1.3 s ($P< 0.05$, n= 4). Although the effect of 1μM SEA0400 on the rate of decay of the caffeine-induced $[Ca^{2+}]_i$ transient was only a fraction of that observed with 10 mM $NiCl_2$, it was clearly detectable. However, these results suggest that the NCX-blocking effect of SEA0400 may be relatively moderate when $[Ca^{2+}]_i$ is elevated.

5.2 Evaluation of intracellular Ca^{2+} changes during type 1 diabetes in rabbit myocytes

5.2.1 Changes of intracellular Ca^{2+} transients and cell shortening in the alloxan-induced diabetic rabbit myocytes

Since the mechanisms that underlie diastolic dysfunction observed in diabetes are not well understood, we tested the hypothesis that diastolic dysfunction is associated with impaired myocardial Ca^{2+} handling, NCX and/or SERCA function in the animal model of type 1 diabetes. As expected, alloxan-treated rabbits displayed hyperglycemia within 24 h after injection, which persisted during the 3 week observation period (5.8 ± 0.4 and 21.5 ± 1.5 mM at baseline and 3 week after alloxan injection, respectively; n = 10, $P < 0.05$). In contrast with controls, alloxan-treated rabbits did gain weight slower. Although alloxan-treated rabbits were insulin deficient, they did not require insulin injections to survive; they remained alert and responsive during the observation period after the onset of diabetes. To record $[Ca^{2+}]_i$ transient, myocytes were stimulated at a constant frequency of 1 Hz through a pair of platinum electrodes. After stabilization period $[Ca^{2+}]_i$ transient as fluorescence signal, and contractile function as cell shortening were measured in steady-state condition. Groups were compared on percent scale, after taking the mean value of the healthy control cells as 100 %. Calcium transient morphology is summarized in Figure 7. Both Ca^{2+} transient amplitude and diastolic Ca^{2+} level, as reflected by Fluo-4 fluorescence signal, tended to be higher in cells from type 1 diabetic animals (100±9 vs. 110±8%, and 100±9 and 120±12%, n=9-12). Ca^{2+} transient decay time (C) in diabetic myocytes was significantly larger in cells from diabetic animals compared to the healthy animals (100±4,8 and 121±6,5%, n=9-12). Despite the elevated Ca^{2+} transient, cell-shortening measurements (D) revealed a significant impairement in contraction function in diabetic cells (100±7% and 72±11% n=10).

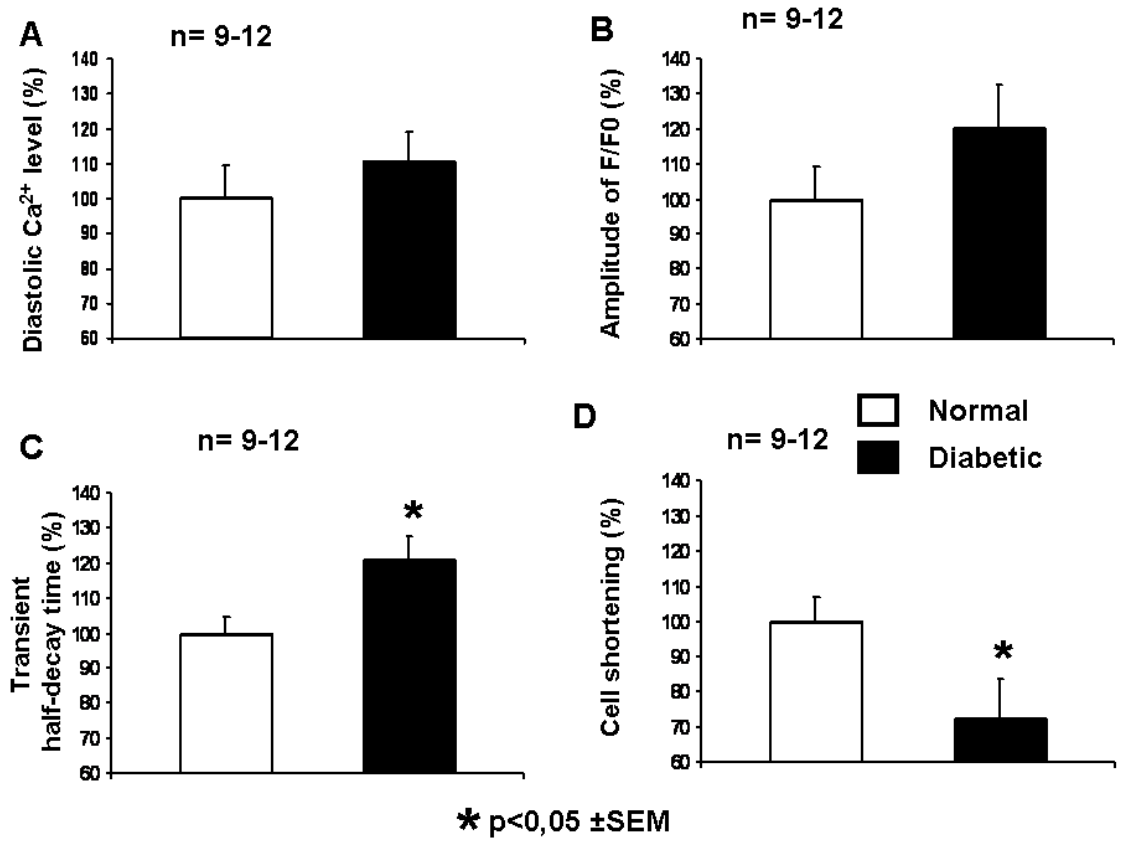

Figure 7 Differences in $[Ca^{2+}]i$ transient and cell shortening of myocytes from control and experimental type1 diabetic rabbits. (B) amplitude of calcium transients, (A) diastolic calcium levels, (C) changes of calcium transient decay constant, and (D) cell shortening measurements Bars represent means ±SEM, and n represents the number of experiments *(p<0,05).*

5.2.2 Comparison of the effect of partial NCX block by SEA0400 on intracellular Ca^{2+} transient and cell shortening in normal and diabetic rabbit myocytes

The myocytes from normal and alloxan-treated groups were field stimulated at a constant frequency of 1 Hz and superfused with normal Tyrode solution. After establishing steady-state contractions and $[Ca^{2+}]_i$ transients, the perfusion was switched to the solution containing 0.3 μM of SEA0400, and a period of 5 min was allowed to develop full drug effect. Original recordings of the intracellular Ca^{2+} transients and cell shortening before and after administration of 0.3 μM SEA0400 are presented in Figure 8. Results show that partial NCX block alters neither the amplitude of Ca^{2+} transient nor diastolic Ca^{2+} level. However, administration of SEA0400 resulted in an increased duration of half-decay time in diabetic myocytes but not in cells from healthy animals. Cell shortening showed an (Fig 8B) increased amplitude in both groups (Fig 8C-D) in response to SEA0400. It must be noted that these experiments were carried out using time matched experimental design, thus the effects of SEA0400 must be related to the spontaneous time dependent changes observed in the

corresponding control group (ie both healthy and diabetic cell populations with and without SEA0400). In other words, we apply between subjects design instead of using within subject design, which results in considerably lower statistical power. However, in this way we can avoid false negative or positive effects that could be due to the spontaneous changes of the measured parameters during the time course of the experiments.

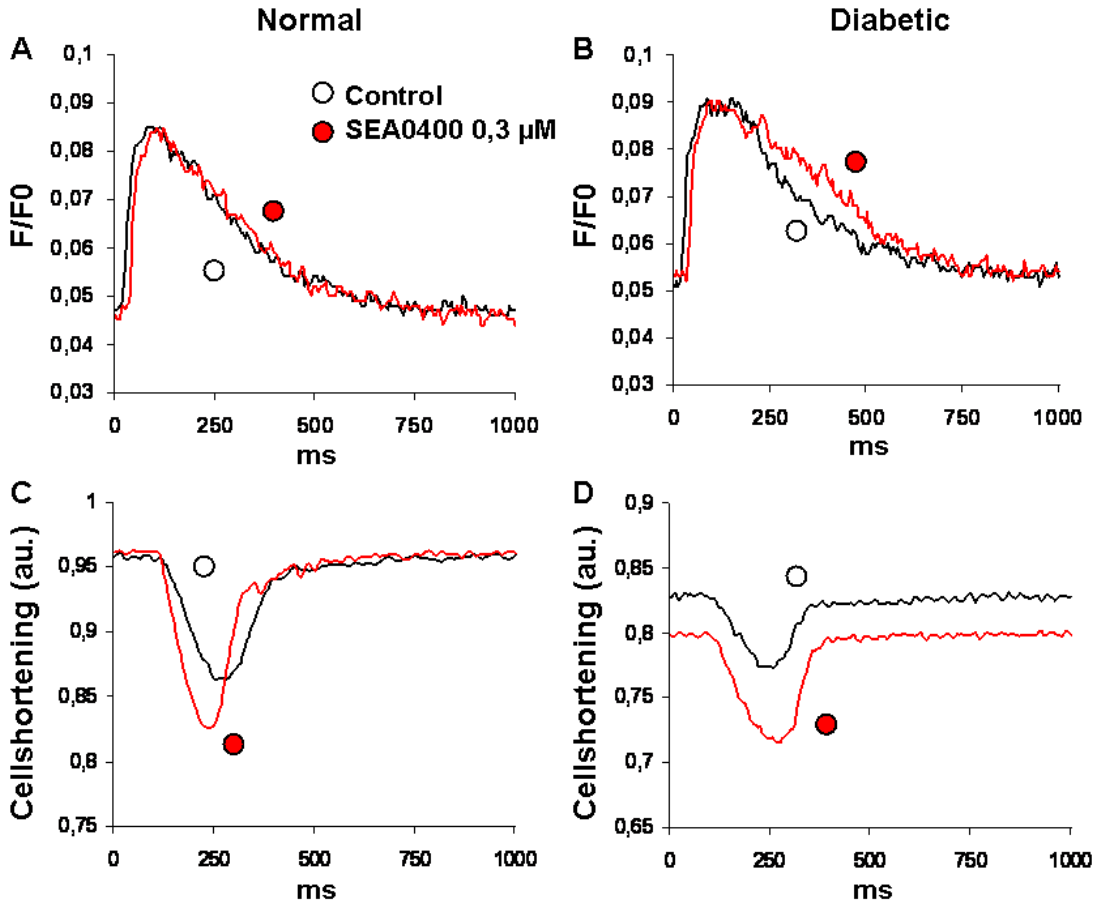

Figure 8 original recordings show the effect of partial NCX block on the intracellular Ca^{2+} transient and cell shortening in the presence of SEA0400 (0,3 µM). (A, C) Cytosolic free $[Ca^{2+}]i$ and cell shortening recorded from normal (non-treated) rabbit ventricular myocyte before and after SEA0400 (0,3 µM). B and D panels show results of a similar experiment using isolated myocytes from alloxan-treated rabbits. Stimulation frequency was constant (1 Hz). Cytosolic free Ca^{2+} concentration is expressed as a fluorescent ratio (F/F0), cell shortening is given in arbitrary units (AU). Recordings were made from the same cells before (open circle) and 5 min after (red filled circle) the application of SEA0400.

Figure 9 A-D summarizes the differing effects of SEA0400 in cells from healthy and diabetic animals according to the above considerations. While there were no effect on diastolic Ca^{2+} level in response to partial NCX inhibition (in normal: -7,9±10,2% before and -4,7±14,1% after, in diabetic: -4,3±12,2% before and 4,2±13,9% after), the amplitude of the Ca^{2+} transient showed a moderate increase in the diabetic group after application of SEA0400 (normal: -2,9±8,4% before and 5,1±8,9% after, diabetic: -1,9±8,4% before and 11±14,4% after).

This was accompanied by a moderately increased amplitude of cell contraction as shown in Figure 9D contraction amplitude (normal: -0,9+8,4% before and 22,7+3,9% after p=0,050, diabetic: -0,7+8,6% before and 15,3+15,2% after). In sharp contrast to these parallel changes of the Ca^{2+} transient and cell shortening in diabetic group, the increased cell contraction in response to SEA0400 occurred apparently without any underlying change in Ca^{2+} transient in the normal group (normal: -2,9±8,4% before and 5,1±8,9% after). It is very hard to interpret this finding, because it is generally accepted that in normal healthy myocytes the increase of the contractile force should be, at least in part, the consequence of the elevated Ca^{2+} transient.

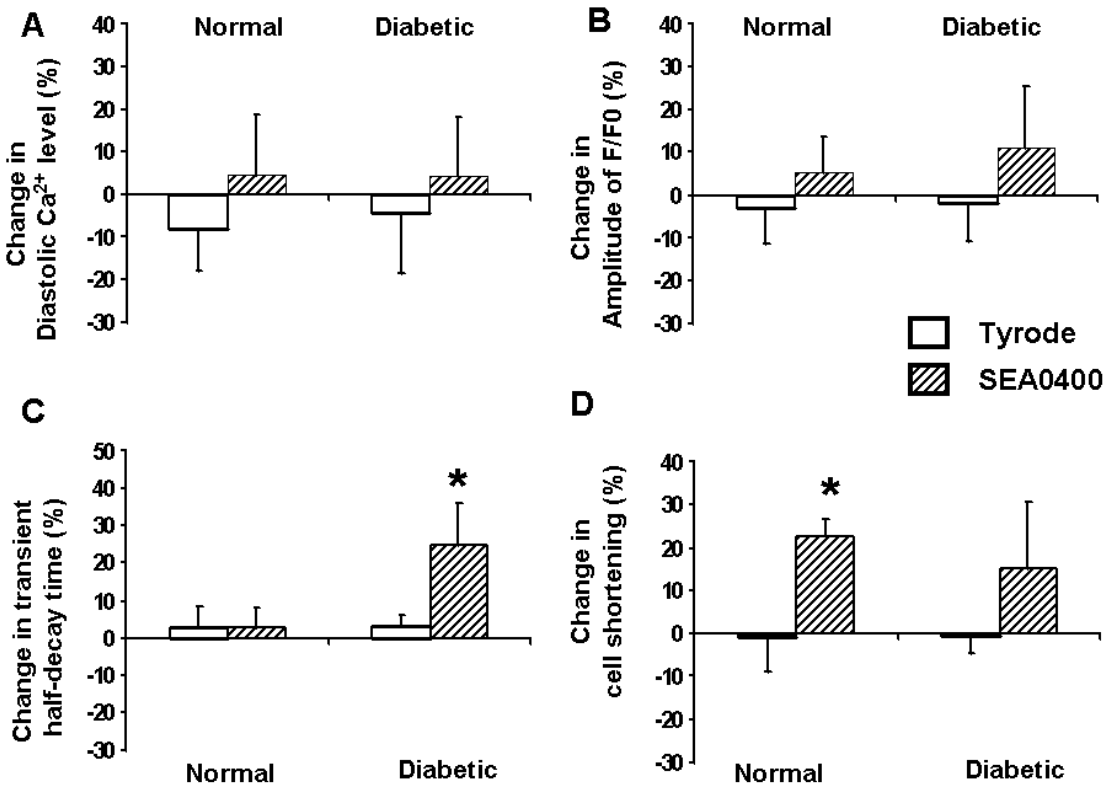

Figure 9. Average results of SEA0400 on transient parameters and cell shortening in field stimulated myocytes from simulated diabetic rabbit. A: Diastolic Ca^{2+} level, B: amplitude of $[Ca^{2+}]_i$ transient, C: half decay time of Ca^{2+} transient, D: cell shortening. Open (Tyrode) and filled (SEA0400) columns represent mean data±S.E.M obtained with the control (n=9) or alloxan-treated (n=10) groups. Asterisks indicate significant differences (P<0.05) between then 0,3 μM SEA0400-treated and the Tyrode groups.

Although increased sensitivity to Ca^{2+} of the contractile machinery could be a possible explanation, it is hard to assume that this would occur after partial inhibition of NCX. Figure 9C shows that the mild increase of the Ca^{2+} transient after application of SEA0400 was also accompanied by a significant lengthening of the half decay time of Ca^{2+} transient (103,1±2,6 ms before and 124,7±11 ms after p= 0,043, n=5). There was no similar effect in the normal healthy group (102,7±5.6 ms before and 102,6±5,2 ms after, n=7), indicating again the altered consequences of NCX inhibition in the diabetic cells.

5.2.3 Analysis of the effect of rest decay in normal and diabetic cells

As depicted in Figure 10 steady state kinetics show a much different time course in cells from diabetic animals. In this protocol cells were stimulated at 1 Hz. Stimulation was stopped for 1 minute, after which again continued. In both groups the amplitude of the first Ca^{2+} transient following the rest period was higher than the following ones, indicating that there was no significant Ca^{2+} loss from the cell during the rest period (Fig10A,B). The smaller 2nd and 3rd transients indicate a temporary decrease in the SR Ca^{2+} load, as a consequence of increased Ca^{2+} extrusion during the first contraction cycle. However, the rest of the time course showed rather different characteristics. As seen in Fig 10C, compared to the healthy group, the refill of the SR lasted much longer in the diabetic group, because (1) at the end of the rest period the SR Ca^{2+} load (as reflected by the Ca^{2+} transient amplitude) was lower, and (2) the final steady state Ca^{2+} level was higher in this group (see also Fig. 7).

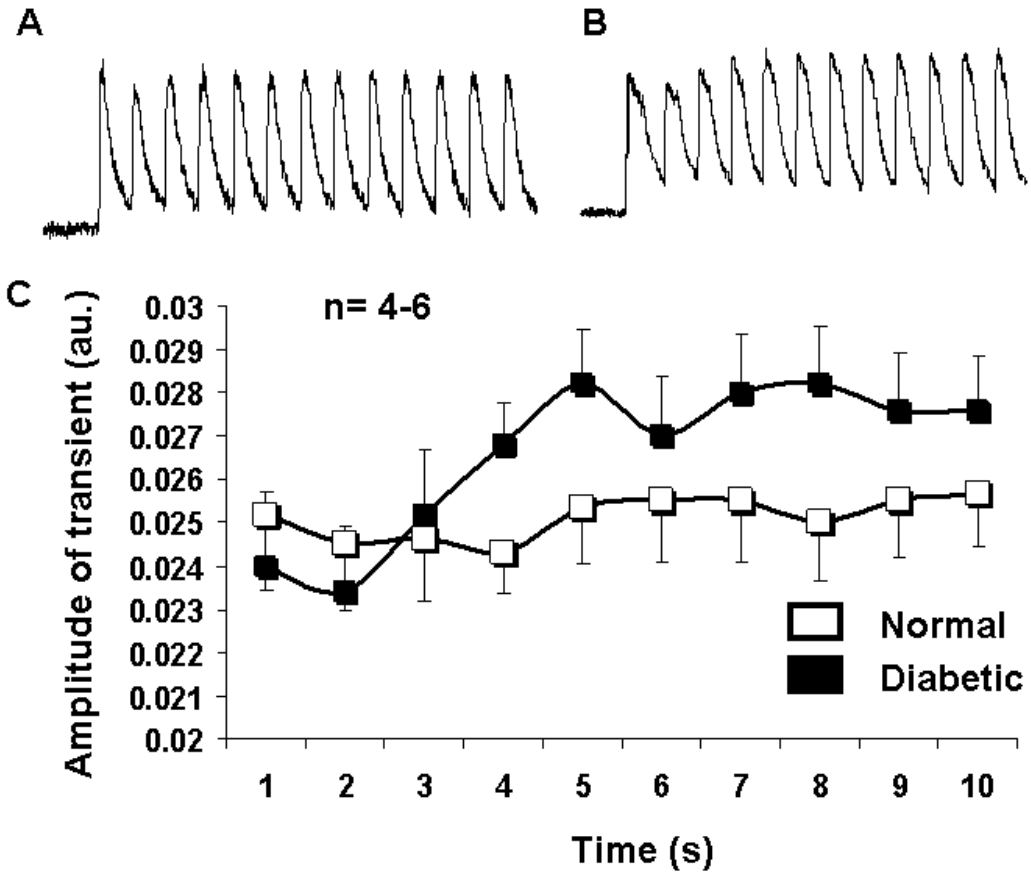

Figure 10. Effect of a pause period in pacing on intracellular free calcium concentrations and Ca^{2+} transient recovery in experimental diabetic myocytes. Representative recordings obtained from normal (A) and diabetic (B) rabbit myocytes under control conditions after 1 minute non-stimulated period by applying 1Hz field stimulation. (C) Original recordings show the recovery from refractoriness under control conditions. Solid lines are the averages mean±SEM, n=4 -6)

5.2.4 Effect of NCX inhibition on the rest decay protocol

The rest decay protocol was repeated in the presence of SEA0400. Results, summarized in Figure 11 show, that while in the healthy group partial NCX inhibition with 0,3 μM SEA0400 only slightly affected the recovery with a small decrease in the final SR Ca^{2+} load (the difference is increasing in time), it exerted a more pronounced effect on the diabetic group, where the whole curve was shifted down and the effect was greater in the first part of the recovery.

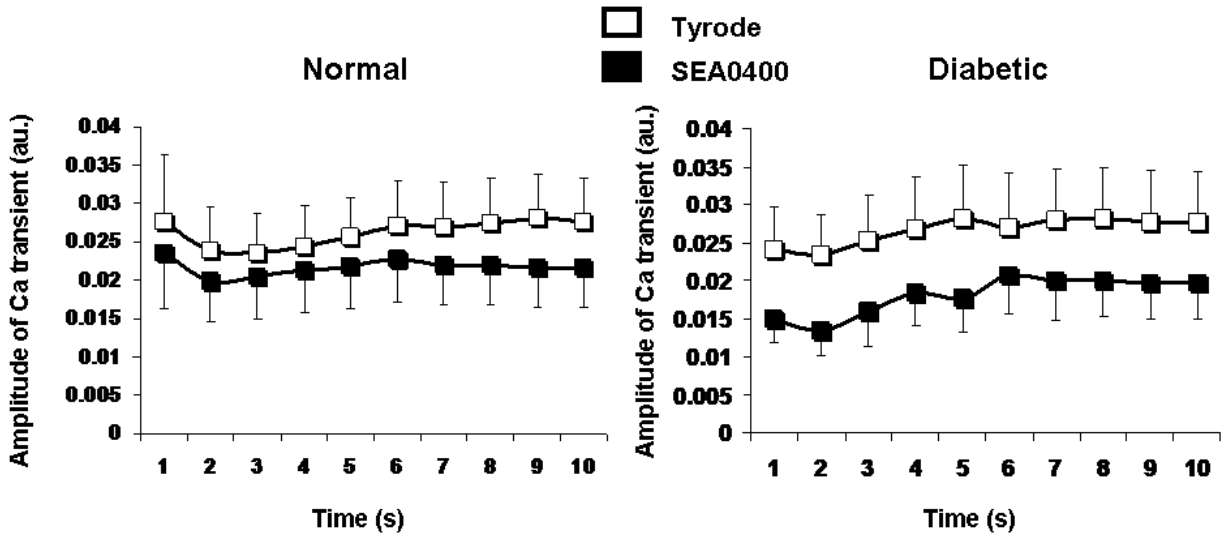

Figure 11. The effect of SEA0400 treatment on the recovery of the Ca^{2+} transient following a 1 minute rest period. Averaged data for untreated (□) and treated (■) (0.3 μM SEA0400) cardiomyocytes from healthy (left panel) and diabetic (right panel) rabbits. (Mean±SEM, (n=5-7).

These results indicate, that though there was only a slight difference between the 1st Ca^{2+} transients during the rest period and/or the refill (see Fig 10), the net Ca^{2+} flux via NCX, as revealed following partial NCX inhibition, is significantly altered in diabetic cells.

5.2.5 Frequency dependent changes in the Ca^{2+} handling

Frequency dependent alterations of the myocardial Ca^{2+} handling are characteristic in different species and cardiac diseases. We tested the possibility that diabetic alterations are accompanied with changes in the frequency dependence of the Ca^{2+} handling. After increasing the stimulation frequency from 0.5 to 2 Hz in our experiments we have found a mild elevation in the diastolic Ca^{2+} level in both the normal and diabetic group (Fig. 12). However, in contrast with our expectations, with the increasing frequency the Ca^{2+} transient amplitude increased neither in normal nor in diabetic cells, indicating that in our experiments the increased Ca^{2+} transient was purely due to the elevated diastolic Ca^{2+}. Similarly to the

earlier protocol, we also repeated the frequency dependent test with and without SEA0400 by applying time matched experiments.

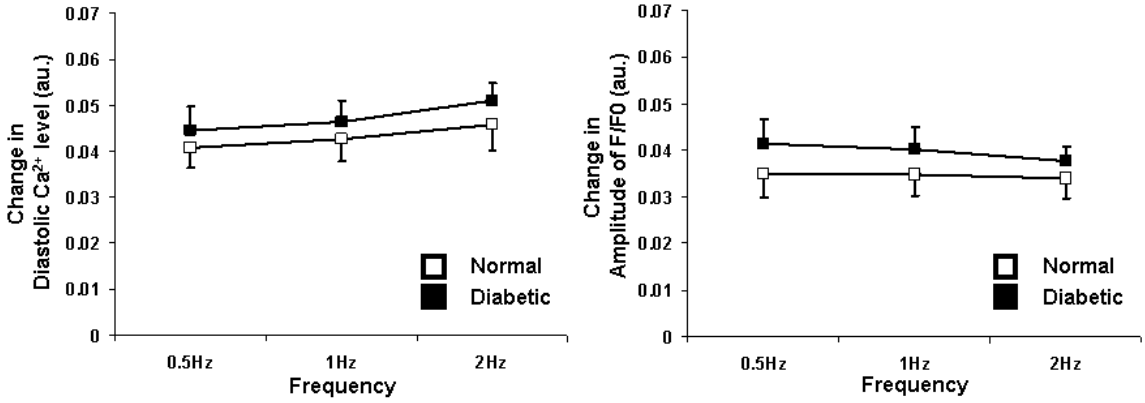

Figure 12 Frequency dependent changes in Normal and Diabetic rabbit myocytes. This figure shows that the response of the diastolic Ca^{2+} level and transient aplitude. The effect of increasing pacing frequency (from 0,5 to 2Hz) increased the diastolic $[Ca^{2+}]_i$ and decreased amplitude of $[Ca^{2+}]_i$ transient in both studied groups.

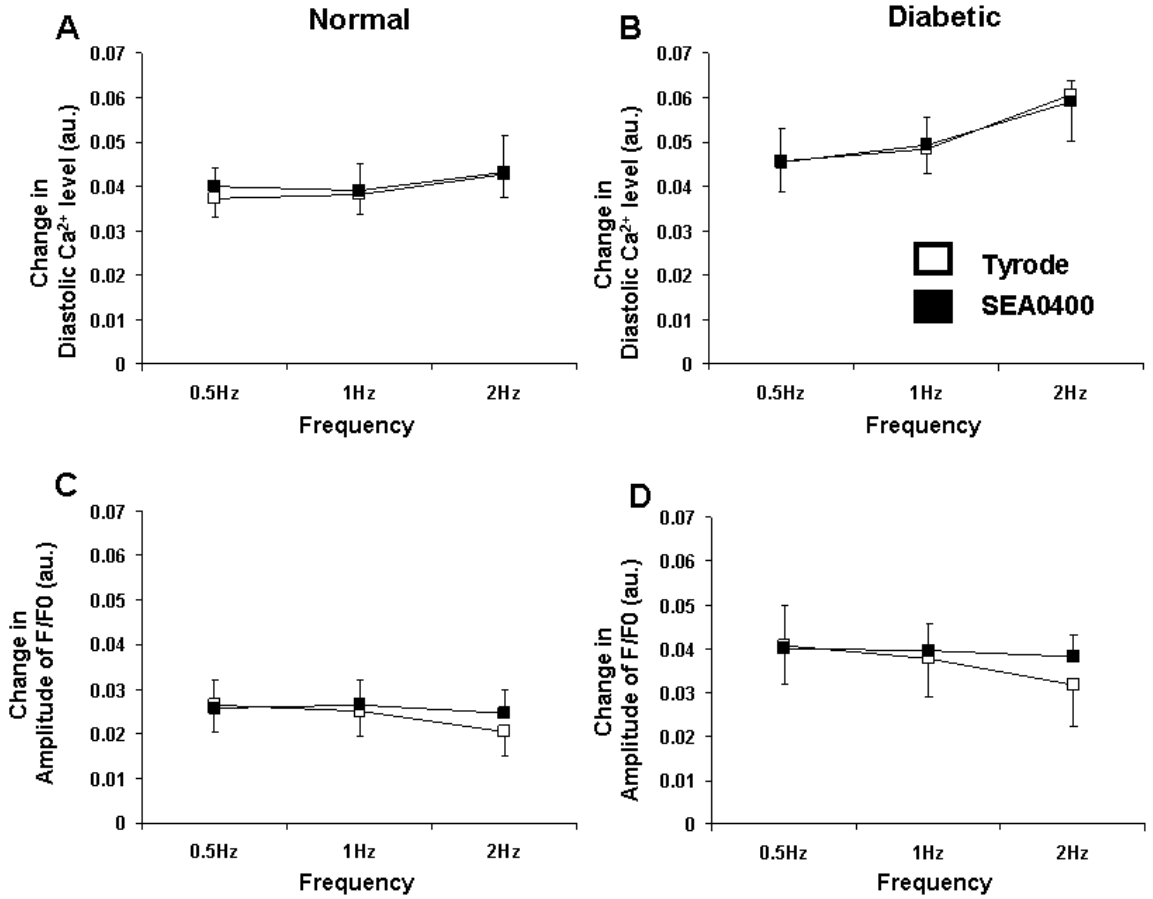

Figure 13 This figure shows frequency dependent effect of SEA0400 in diastolic calcium levels (A, B) and amplitude of calcium transients (C, D). In Ca^{2+} transient amplitude were found that efficiency of SEA0400 to be dependent on the rates of pacing. Panel C and D shows SEA0400 have a moderately but higher efficiency under 2Hz pacing in both studied group.

As shown in Figure 13 application of SEA0400 did not cause any change in the frequency dependent behavior of the diastolic Ca^{2+} level in neither of the groups, while it tended to

increase the amplitude of Ca^{2+} transient in both groups at 2 Hz, with a bigger effect in case of diabetic cells, which is in line with the results of the protocol in Figure 9. In contrast, Ca^{2+} transient amplitude after SEA0400 tended to decrease in the diabetic group.

5.3 Herpesvirus-mediated delivery of a genetically encoded fluorescent Ca^{2+} sensor to canine cardiomyocytes.

5.3.1 Morphological changes of cultured cardiomyocytes

Using the described method for isolation of adult dog left ventricular myocytes, we routinely obtained a high yield (more than 80%) and high (more than 80%) percentage of rod-shaped myocytes, that were suitable not only for acute functional studies but, more importantly, for short-term culture and gene transfer. Figure 15a shows a trans-illumination image of freshly isolated and 1-day-old cultured cardiomyocytes from the left ventricle. To establish optimal surviving conditions several culture conditions were tested, based on microscopic evaluation of changes in cellular morphology during four days of culture. Cultured cells were used 1-3 days after isolation. During this period, visible minor changes in cell shape and cross-striation could be observed. Figure 15b shows representative photographs of canine myocytes over time in primary culture. Features typical of acutely isolated (Day 0) cells were the rod shape with rectangular stepped ends and clear cross-striations. After 1 day (Day 1) in culture, the cells were still rod-shaped with clear cross-striations; however, the ends of the cells started to become slightly rounded in appearance. After 3 days (Day 3) in culture, cells remained rod-shaped and cross-striated, and the main change was that cell ends became progressively more rounded (see Table 1 for cell survival rates).

		Day 0	Day 1	Day 2	Day 3	Day 4	Day 5
Control	Average (%):	100	60,0	44,9	4,3	2,8	2,2
	Standard error:		6,0	8,4	0,5	0,3	0,3
Virus infected	Average (%):	100	85,5	69,2	12,8	3,1	1,3
	Standard error:		4,7	9,3	3,7	1,5	0,6

Table 1 This table shows the survival of non-infected and virally infected cells from day 0 to day 5. It can be seen that virally infected cells exhibit slightly better survival than non-infected cells, for which the reason remains to be ascertained.

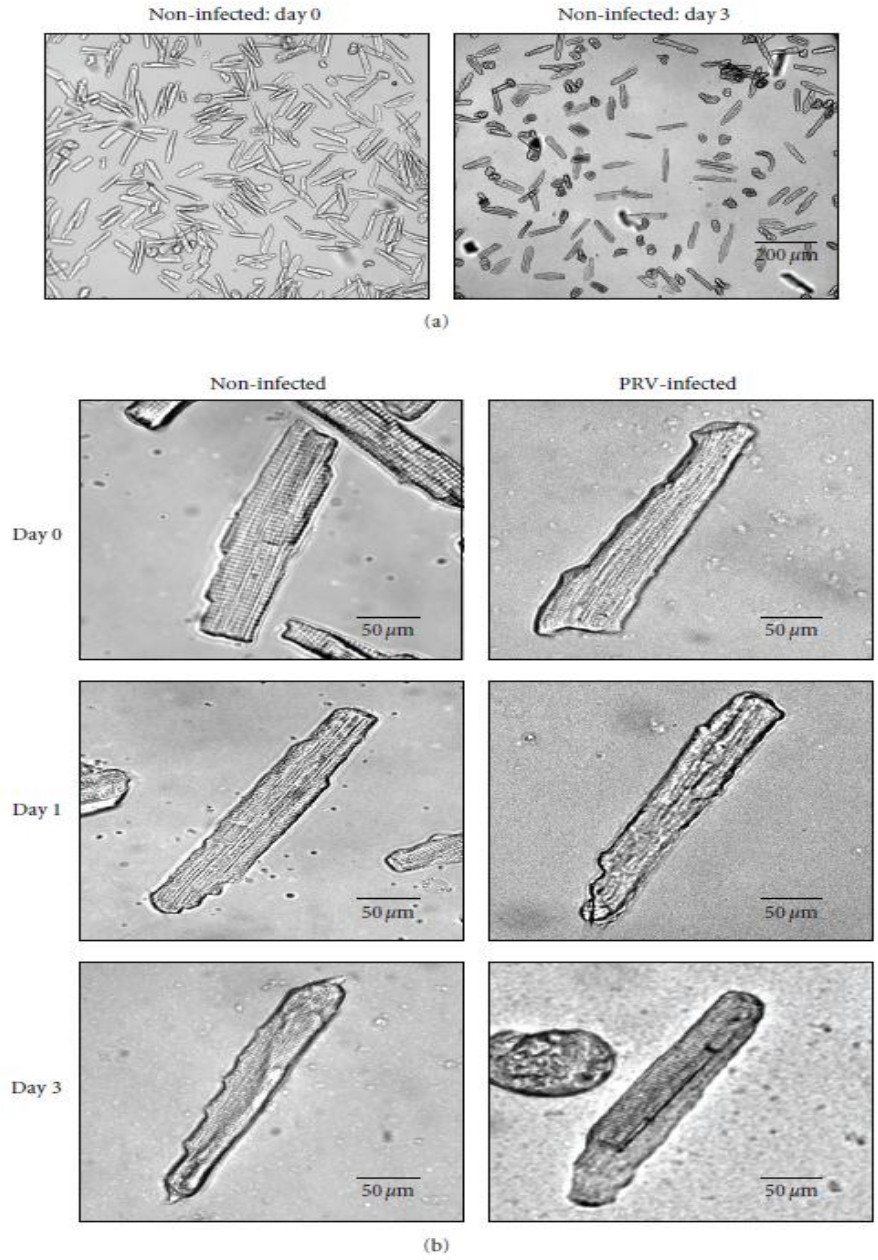

Figure 15: Representative low and high magnification trans-illumination of adult dog myocytes after isolation (day 0) and 1–3 days of culture (day 1, day 3). (a) shows the yield of the myocytes before and one day after culturing and infection. The high-magnification transillumination (b) shows the morphology of adult dog myocytes after isolation (day 0) and 1–3 day of culture (day 1, day 3) and the morphological changes of living cells, versus the culturing time from non-infected (right) and the virus-infected groups (left). After one day plated myocytes more than 80% displayed a rod-shaped morphology and healthy cross-striation. After 3 days (day 3) in culture, cells remained rod-shaped and partially cross-striated, and the main change was that cell ends became progressively more rounded.

5.3.2 Efficacy of virus infection in cultured cardiomyocytes

Survival rates were found to be dependent on the isolation procedure, density of the attached myocytes and the applied virus titer. Intriguingly, a higher total number of viable cells were observed on the laminin-coated surfaces after plating in CCTI supplemented

medium. As respective panels of Fig 15 and 16 (upper panel) shows, even after three days, the cell culture contained a substantial number of good quality cells both in the control and virus infected groups. Surprisingly, a moderately but consistently higher cell survival rate was found in virus infected groups as compared to non-infected groups (not shown). The infection efficiency was found to be 100%, that is 24h post-infection every surviving cells emitted fluorescent signals provided that high dose of virus was used for the infection (Fig 16 bottom panel).

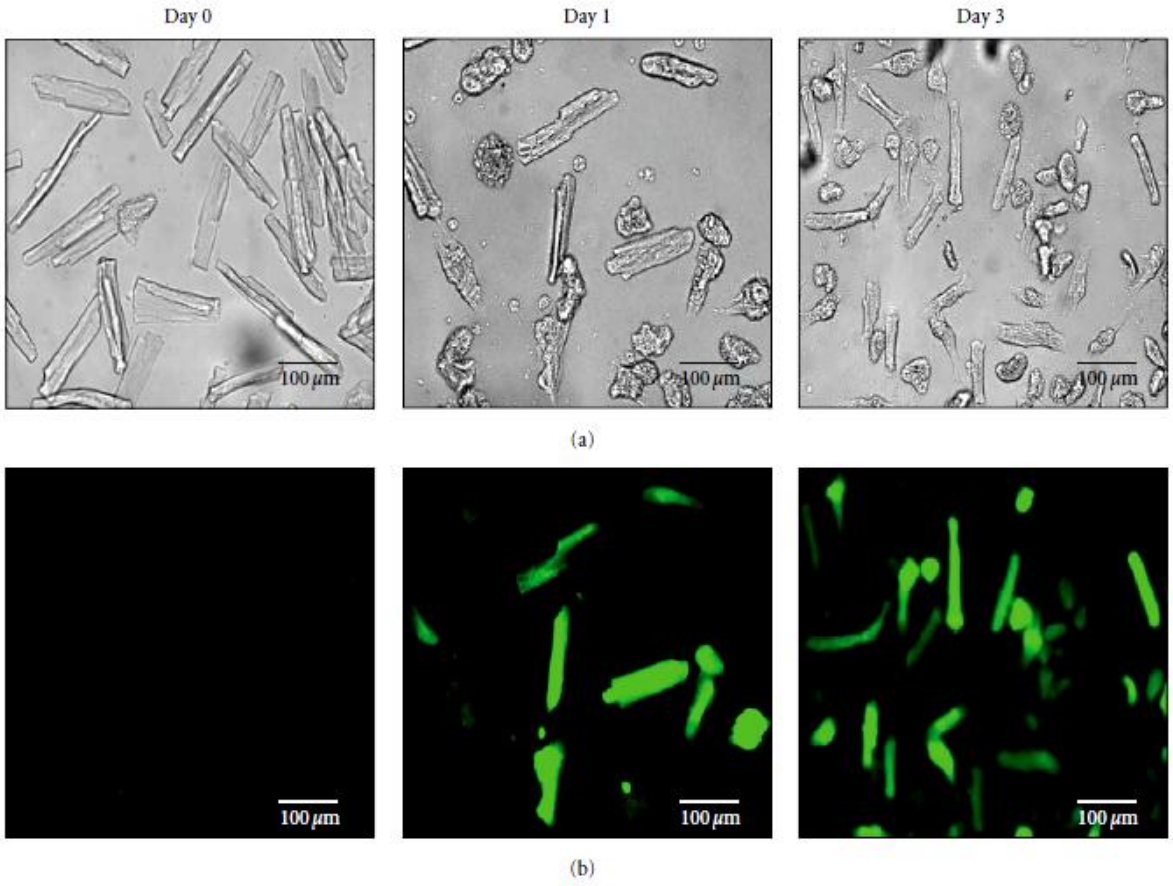

Figure 16: (a) Representative light and (b) fluorescent microscopic images of cell culture, before and after 1 day and 3 days of virus infection. Expression of recombinant pseudorabies-viral troponeon transgenes appeared on high level in cultured adult dog ventricular myocytes. The isolation of adult dog left ventricular myocytes yielded more than 80% living cells. After three days the troponeon expression and the physiological features of survival myocytes was appropriate for the physiological studies.

5.3.3 Whole-cell patch-clamp recordings

The whole-cell configuration of the patch-clamp technique was used to record the transient outward I_{to} current. I_{to} was chosen as a physiological assay because it is a large current that can be measured relatively easily in isolated canine ventricular myocytes. The

current was activated by 300 ms long depolarizing voltage pulses from the holding potential of -90 mV to test potentials ranging from 0 to $^{+}$60 mV with a pulse frequency of 0.33 Hz.

The amplitude of I_{to} was measured as the difference between the peak and the sustained current at the end of the voltage pulse. Figures 17A shows typical recordings of I_{to} measured after one (Day 1) and three days (Day 3) of culture either in control (top panels) or virus infected cells (bottom).

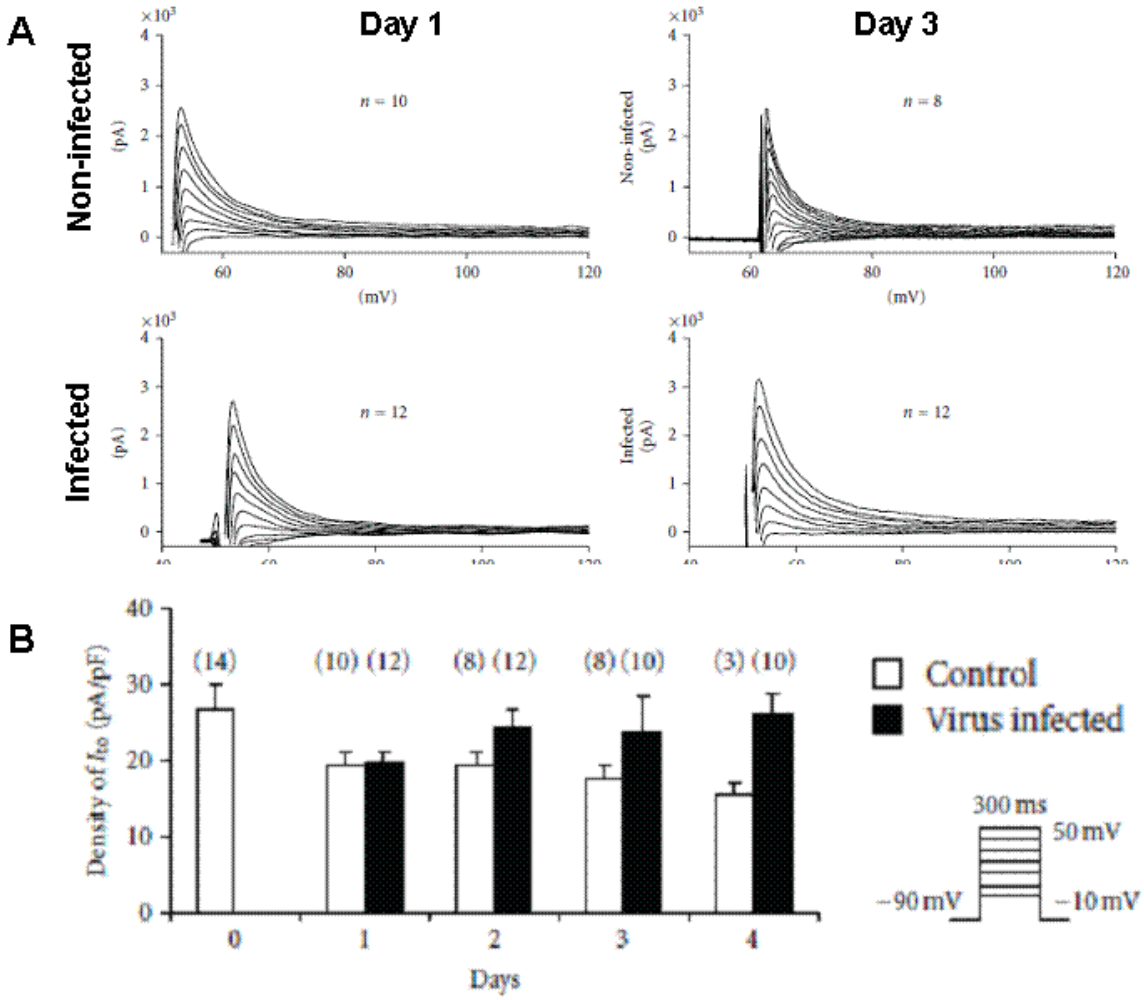

Figure 17: (A) Transient outward K current (I_{to}) recordings from control and from virus-infected myocytes after 1 and 3 days of culture. Inset shows applied voltage protocol. (B) shows the Ito current densities from control and from virus-infected myocytes after 1 to 4 days long culture. Data represent means ± SEM, and n represents the number of cells.

Figure 17B summarizes all I_{to} measurements performed after 0-4 days of culture in both groups. As the corresponding panels of Figure 17 show, the amplitude of the I_{to} was reduced by less than 10% in virus infected myocytes (VM) compared to control non-infected cells (CM) even after 4 elapsed days. The I_{to} kinetics (activation and inactivation properties) were

also not altered significantly by the virus infection. Moreover current amplitude was somewhat larger in PRV-infected cells compared to that of observed in control cells. Mean I_{to} density (Fig. 17B) was similar for CM and VM cells after 1 day. The I_{to} current density in VM changed in four days from 19.6 ±1.4 to 24.6±2.6 pA/pF (n=10-12), which corresponds well with that observed in CM (from 19.3±2.1 to 17.1±1.5 pA/pF, n=8-10). Although mean I_{to} density of several-day-old (2, 3, 4) cultured myocytes was significantly larger in VM than CM.

5.4.4 Parameters of intracellular Ca^{2+} transients and contractility in PRV-infected myocytes

Myocytes were stimulated at a constant frequency of 1 Hz. Similar to the I_{to} measurements, steady-state Ca^{2+} transient and contractile function (cell shortening) were measured and compared on a daily basis, both in the infected and the control cell populations. Original recordings of $Ca^{2+}{}_i$ transients and cell shortening before and after virus infection are presented in Figure 18.

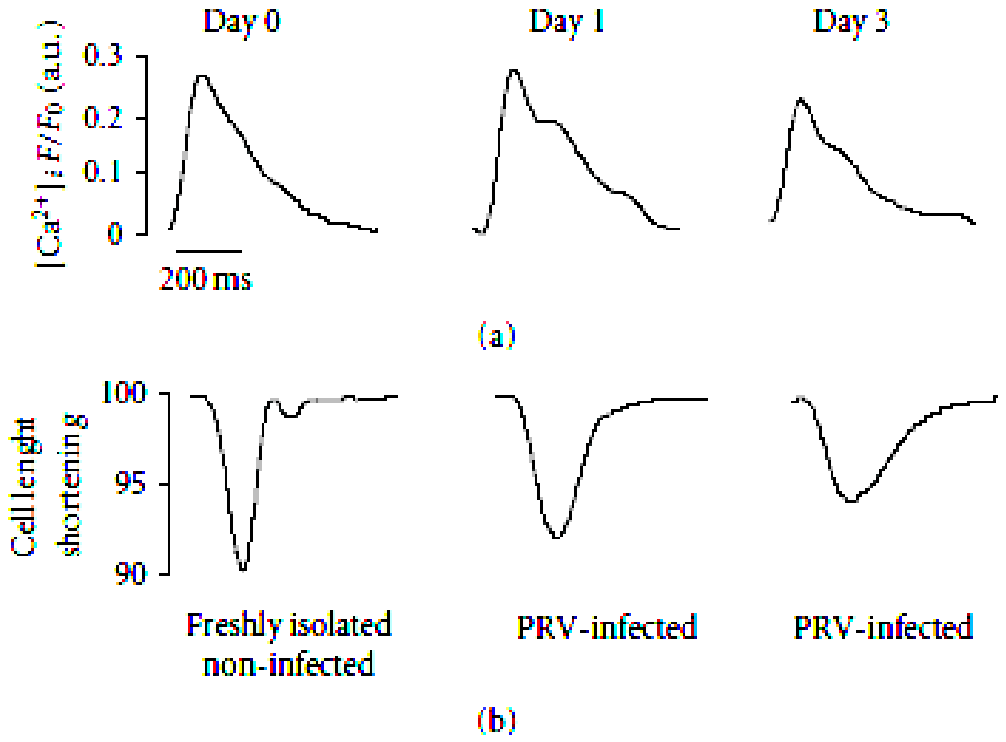

Figure 18: Original Ca^{2+} transients and cell shortening recording in cardiomyocytes cultured for 1 and 3 days. The top panel shows the Ca^{2+} transients and bottom panel the parallel changes in cell length.

The kinetics of the Ca^{2+}_i transient was rather distorted in culture, but did not significantly alter following viral infection. As summarized in Figure 19, we did not find statistically significant difference between the two groups in either the amplitude of Ca^{2+} transient (a) or the diastolic Ca^{2+} levels (b). Moreover, the decay time of the Ca^{2+} transient was significantly longer in the non-infected myocytes than in the virus infected group (c) after two or three days in culture. Conversely, in the virus-infected groups decay time was similar to that in freshly isolated cells. These results suggest that the non-infected cell population may have lost some of their calcium removal mechanism. The cell-shortening measurements (d) show a significant decline in non-infected cell culture after 1 and 3 days.

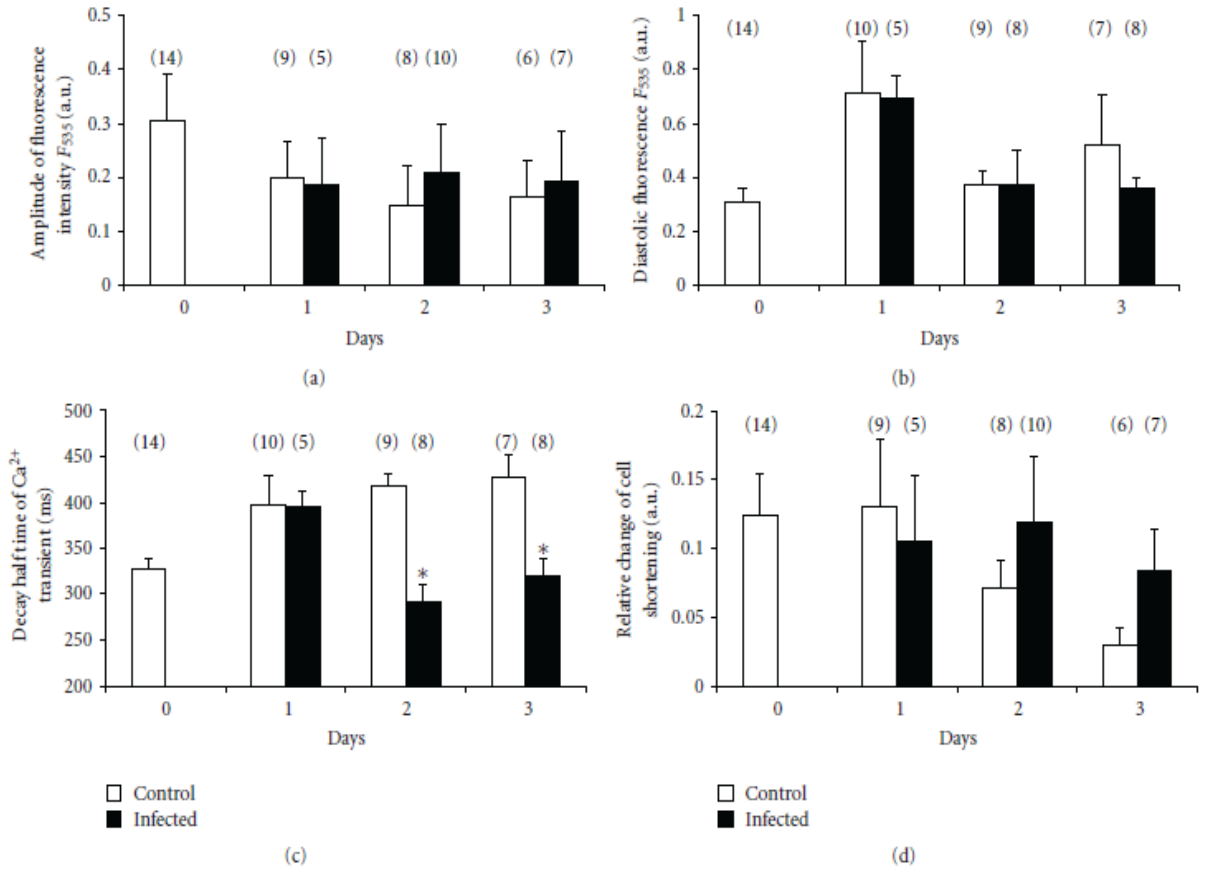

Figure 19: This figure shows several parameters of intracellular free calcium transient such as (a) amplitude of calcium transients, (b) diastolic calcium levels, (c) changes of calcium transient decay constant, and (d) cell-shortening measurements from recordings from control and from virus infected myocytes after 1 to 3 days long culture. Bars represent means ± SEM, and *n* represents the number of experiments.

5.4.5 Functionality of FRET-based calcium sensor

Freshly isolated ventricular myocytes were infected with the virus following 4h plating and fluorescence could already be detected within 16h. The functionality of the transferred gene was verified by monitoring $[Ca^{2+}]_i$. Figure 20 shows two typical fluorescence signal emissions measured in troponenon-expressed cells obtained at 485 nm and 535 nm excitation (upper panel). The lower panel shows the ratio of the citrine and CFP emitted signals representing the changes of the $[Ca^{2+}]_i$ levels in the studied cells. This measurement clearly shows that virally-encoded troponenon retained its ability of indicating $[Ca^{2+}]_i$ levels in cardiomyocytes.

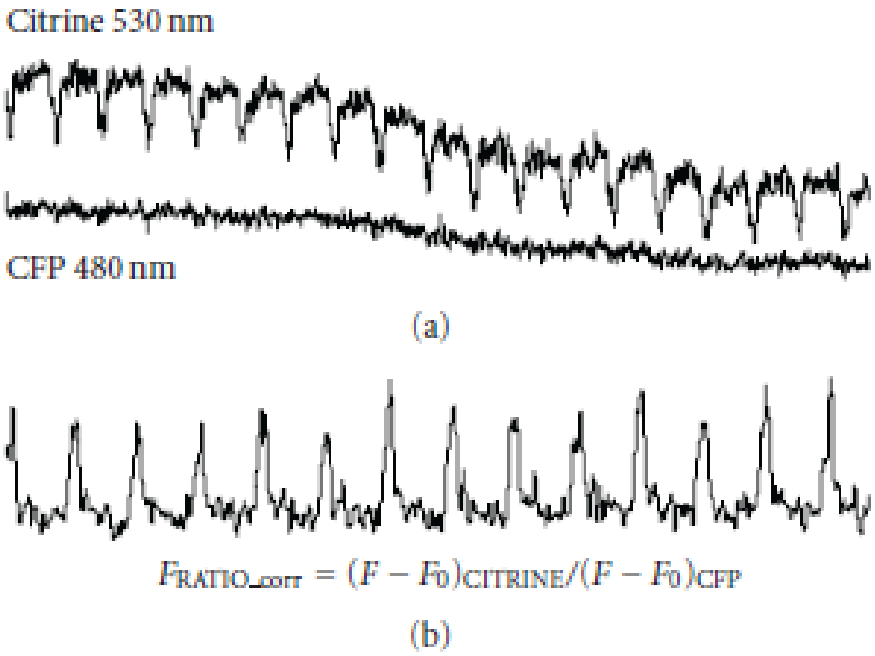

Figure 20: (a) Original recordings from cells expressed troponeon at the excitation wavelength of (a) 485 and 535nm and (b) the characterized calcium transient by ratio of the fluorescence intensity (FCITRINE 535 / FCFP 485) from one day after infection.

6. DISCUSSION

6.1 New challenges in the field of Ca^{2+} signaling research

It is well established that the Ca^{2+} ion has many important functions in living organisms in all fields of biology. It is not only an effector for vital cell functions such as cell contraction or exocitosis, but also plays crucial role in regulation of activity of metabolic enzyme systems and many signaling pathways [4]. Specifically in cardiomyocytes, since the early experiments demonstrating vital role for Ca^{2+} in excitation contraction coupling, there have been numerous discoveries regarding additional important functions for Ca^{2+} in subcellular signaling [2]. The introduction of Ca^{2+}-sensitive fluorescent dyes more than twenty years ago and their permanent improvement [10] enabled investigators to gain unprecedented insights into the mechanisms of cellular signalling. The dynamics of $[Ca^{2+}]$ changes at the whole cell level and in well-defined subcellular compartments in excitable cells during the course of membrane depolarization can now be much better understood in the context of disease processes such as cardiac arrhythmias and heart failure or diabetes.

In the living cells Ca^{2+} ion has a unique feature that it exerts multiple actions even within the same cell at the same time, depending on type of receptors or enzymes present in the cell. Furthermore, recent research underlines that in addition to multiple functions, spatial and temporal separation of local Ca^{2+} signals even within the same cytosolic compartment may be crucial in normal cellular function [42]. Indeed, it has been shown that disintegration of this complex spatiotemporal signaling system is characteristic during development of cardiac diseases [43], which emphasizes the needs of a more specific and targeted detection of local Ca^{2+} signals, in order to understand disease process in cardiac myocytes and also to explore new potential therapeutic targets. In this field, application of the FRET based methods can provide us with a useful tool in the Ca signaling research.

6.2 Effect of SEA0400 on caffeine induced Ca^{2+} transients in canine cardiomyocytes: validation of SEA0400 as a tool to study the Ca^{2+} homeostasis

Earlier reports on the effect of SEA0400 on Ca^{2+} handling [41, 44-46] are nonuniform and in some cases the findings are unexpected. These controversies may be due to species-specific differences in Ca^{2+} homeostasis and Ca^{2+} handling (i.e. the relative role of NCX in the maintenance of physiological Ca^{2+} levels), or due to inherent properties of SEA0400. For example, earlier studies [41] show that SEA0400 may have different efficacy in inhibiting NCX depending on the intracellular ionic composition. Specifically, high intracellular Ca^{2+}

has been shown to counteract the blocking effect of SEA0400 on NCX [47]. These results may question the use of SEA0400 as an applicable tool in the Ca^{2+} handling research. Therefore, in our first experiments we characterized the NCX inhibiting effect of SEA0400 in an experiment where a high and long lasting intracellular Ca^{2+} level is achieved by application of 10 mM caffeine. In this experimental setting the extrusion of Ca^{2+} from the cell is achieved only via the NCX, thus in this model the activity of NCX can be studied accurately. Under these conditions, inverse Ca^{2+} dependent NCX inhibiting effect of SEA0400 can be assumed to be maximal, thus in the experiments on the diabetic rabbit cells the actual degree of NCX block is presumably at least as large as in this caffeine experiment. According to our results, the effect of 1 μM SEA0400 on the rate of decay of the caffeine-induced Ca^{2+} transient was only a fraction of that observed with 10 mM $NiCl_2$ (20%) These results suggest that the NCX-blocking effect of SEA0400 may be relatively moderate when $[Ca^{2+}]_i$ is elevated. It must be noted that weak inhibition of NCX in our experiments is not necessarily a disadvantage, because higher degree of inhibition can easily result in accumulation of Ca^{2+} inside the cell, which would lead to cell hypercontraction or cell death, especially in case of cells from diabetic animals, where the Ca^{2+} homeostasis is already compromised.

6.3.1 Disturbed Ca^{2+} handling in type 1 diabetes

Our second aim was to investigate the altered Ca^{2+} handling of cardiac myocytes in a diabetic animal model, with special emphasis on possible contribution of NCX to altered Ca^{2+} handling during the disease process. Isolated diastolic dysfunction is observed in almost half of otherwise asymptomatic patients with well-controlled diabetes and thus may precede diastolic heart failure. Since the mechanisms underlying diastolic dysfunction observed in diabetic patients are not well understood, we tested the hypothesis that diastolic dysfunction may be associated with impaired myocardial Ca^{2+} handling, NCX and/or SERCA function in an animal model of type 1 diabetes.

Earlier studies have shown that in isolated ventricular myocytes, diabetes resulted in a significant prolongation of action potential duration compared with controls, with after depolarizations occurring in diabetic myocytes [48]. Sustained outward K^+ current and peak outward component of the inward rectifier current were reduced in diabetic myocytes, while I_{to} was increased. It is important to note that there was no significant change in L-type Ca^{2+} current. As L type Ca^{2+} current is a major component in Ca^{2+} cycling, this fact helps to interpret the changes in the Ca^{2+} handling that we observed as a consequence of diabetes. Thus, our goal was to characterize the cellular events associated with diastolic dysfunction in

experimental diabetes mellitus and to explore what role NCX may play in these pathological circumstances.

We were able to reproduce characteristic diabetic alterations, including increased diastolic Ca^{2+} levels (Fig 7) as manifestation of diastolic dysfunction, and reduced cell shortening. However, despite of the obvious signs of disturbed Ca^{2+} handling, the differences between the diabetic and healty cells were not very pronounced in our experiments. Obviously, this is a major limitation of the diabetes model we used, emphasizing the need for development of better experimental models and further extensive research in this field. Interestingly, in our rabbit model, at least at this stage of disease, the loss of contractile force was not associated with reduced intracellular Ca^{2+} transient. The increased Ca^{2+} transient seen in our experiments probably reflects a compensatory mechanism that helps to maintain cellular contractility. Alternatively, decrease of the Ca^{2+} sensitivity of the contractile machinery can also occur as a primary alteration during the disease process.

As one of the most characteristic change in diabetic cells, we found that relaxation of the Ca^{2+} transient was prolonged, which is in line with previous observations suggesting a diminished SERCA function as a consequence of diabetes. Inhibition of NCX by application of SEA0400 further prolonged the Ca^{2+} transient in diabetic, but not in normal cells, suggesting an increased role for NCX in the maintenance of Ca^{2+} homeostasis in diabetic cells. This is also supported by our other finding that SEA0400 increased the Ca^{2+} transient in the diabetic cells, but not in normal cells, indicating that diabetic cells are more sensitive to any perturbation of the Ca^{2+} cycling. On the other hand, SEA0400 also increased the contractile force in the diabetic cells, which may suggest a potential therapeutic possibility for NCX inhibition.

A difficult point in our results is the increased contractility observed in normal cells in response to SEA0400, which was apparently independent of the intracellular Ca^{2+} transient. It is very hard to interpret this finding, because it is generally accepted that in normal healthy myocytes the increase of the contractile force should be, at least in part, the consequence of the elevated Ca^{2+} transient. Although increased sensitivity of the contractile machinery to Ca^{2+} could be a possible explanation, it is hard to assume that this would occur following partial inhibition of NCX. A possible, though rather speculative explanation is that inhibition of NCX can also affect the local submembrane Ca^{2+} levels ($[Ca^{2+}]_{sm}$), which could in turn influence membrane bound enzyme systems involved in signaling cascades, leading to altered Ca^{2+} sensitivity of the contractile system. A possible role for such local $[Ca^{2+}]_{sm}$ changes in

the regulation of cell physiology emphasizes the need for the development of novel methodology to detect Ca^{2+} in specific subcellular compartments.

6.3.2 Rest decay experiments

Kinetics of the development of the steady state conditions in the Ca^{2+} handling after a period of rest can also provide valuable insights into the altered Ca^{2+} handling in diabetes. Cardiac myocytes from different species can behave differently in this test, results depend on the actual balance between the trans-sarcolemmal and SR Ca^{2+} fluxes. Alterations associated with different pathological situations can also affect the equilibrium between these Ca^{2+} routes at rest. Indeed, we found that diabetic cells showed a slower time course of Ca^{2+} refilling kinetics. This occurs in spite of no change in I_{CaL}, which is the main source of Ca^{2+} under these conditions, suggesting that either the reverse-mode NCX and/or the SERCA function is hampered in the diabetic cells.

Regarding the effect of NCX inhibition on the recovery of Ca^{2+} transient after resting period, we found an interesting difference between the behavior of first and final part of the curve in the normal and diabetic cells. Theoretically, the final Ca^{2+} load during this protocol depends on the relative magnitude of Ca^{2+} fluxes via SERCA and forward NCX. Inhibition of NCX would favour the SR Ca^{2+} refilling through SERCA, which would result in increased Ca^{2+} load of the SR and would lead to elevated Ca^{2+} transient. However, our measurements show that the Ca^{2+} load of the cell becomes lower after NCX inhibition in both groups, suggesting a more complex scenario during this protocol. An obvious explanation for this phenomenon would be the involvement of the reverse-mode NCX in the refilling of the cell with Ca^{2+}, which is also blocked by SEA0400. The validation of this hypothesis, however, would require a more thorough investigation. The lower Ca^{2+} transient amplitude at the end of the protocol in the presence of SEA0400 can also be ascribed to the concomitant inhibition of I_{CaL} [41], because of which the final steady state occurs at lower level of cell Ca^{2+} content.

The first part of the curve, however, shows different behavior, with a lower Ca^{2+} transient in the diabetic group. A reasonable, although speculative interpretation can be that inhibition of a certain percentage of NCX reveals an already hampered NCX function in diabetic cells, which results in slower Ca^{2+} refilling. This explanation implies again that reverse NCX may play a role in the beginning of the refilling process. Indeed, the reverse NCX is allowed to work and carry Ca^{2+} into the cell during the first part of the action potential (see Fig 1), but only when the local subsarcolemmal Ca^{2+} is low, a condition that can be met in case of smaller Ca^{2+} transient at the beginning of the curve. Whether this occurs in our case however,

would require a more direct experimental support by measuring subsarcolemmal Ca^{2+} and its impact on Ca^{2+} refilling kinetics.

Another interesting point that we observed in this protocol is that compared to the effect seen in (Fig 8, 9) the Ca^{2+} transient amplitude in the diabetic group changed in the opposite direction after application of SEA0400. These findings may suggest the differing role of NCX in the beat-to beat Ca^{2+} cycle at steady state conditions and during the adaptive changes of the Ca^{2+} handling like in this refilling protocol.

6.4 Delivery of troponeon to cultured cardiomyocytes

The past decade has witnessed an explosive progress of virus-based gene delivery technologies. The reason for this is that, albeit traditional approaches, such as calcium phosphate precipitation, electroporation, or liposome-mediated gene transfer perform excellently in immortalized cells of various origins, they mostly fail in primary cultured cells and under *in vivo* conditions. Viruses had to evolve several means for effective infection of cells that can be employed by utilizing viruses as vectors for delivering exogenous genes to the desired cells. Virus-mediated gene transfer methods have also become applicable experimental tools in cardiovascular research. In this thesis we summarize the advantages and pitfalls of a variety of Ca^{2+} indicators used in some optical technique employed for measuring intracellular Ca^{2+} levels. Recent advances of transgenesis and gene targeting technologies have heralded a new era of studies in cellular physiology to study molecular function using genetically engineered animal models and genetically encoding vector-based gene transfer systems. Several transgenic and gene-targeted models have been generated for the over-expression [49, 50], and genetic ablation of key proteins [51, 52] governing cardiac structure and function. At present, however, in spite of the permanent improvements, techniques for introducing foreign genes to cultured adult cardiomyocytes suffer from substantial limitations, such as relatively low infection efficacy and/or cell surviving rate for the integration of transgenes be delivered [53, 54]. In addition, a number of studies demonstrated that vector associated cytotoxic effects directly affect a number of (electro) physiological properties of the cells [24].

Transfering foreign genes to cardiac cells of living animals is a feasible technique in several animal models; however, performing electrophysiological measurements *in vivo* is not easy, therefore usually *in vitro* electrophysiological techniques are used in cultured cells for this purpose. Similar experiments were performed in a recently published work using cultured human atrial myocytes [55] and myocytes isolated from rat, a species from which producing

long term cell culture is much easier. Gene transfer to cardiac myocytes has been traditionally carried out in neonatal cells. However, these cells undergo differentiation, and as a result, this model is inappropriate for certain experiments since differentiating cells have ionic currents different from those in adult cells. Therefore, *in vitro* transducing of isolated cardiac myocytes can be a useful alternative for investigations of cardiovascular cell physiology and diseases.

Small rodents (such as mouse, rat) are far not ideal for modelling human cardiac diseases like heart failure, myocardial infarction and arrhythmia, since the small rodent heart has distinctly different action potential waveform due to its differing underlying ionic currents [56]. Therefore, in our third study we opted for a canine model, since the dog unlike the mouse and rat models is known to have characteristic action potentials and ionic current similar to those in human [57].

For testing the possible effects of viral infection the transient outward potassium current was chosen because I_{to} is a relatively large current, and is present in all cells. Also, it can be relatively easily measured. The I_{to} gene structure is rather complex. The I_{to} current in canine myocytes resembles human myocytes and has a large conducting pore forming unit Kv4.3 connected with several auxiliary subunits such as KChIP2, KCNE2 and DPPX [58]. Structural changes during culturing ventricular myocytes were also studied [59, 60]. These changes are associated with culturing procedure associated effects, which may change a number of physiological properties of the cells in culture. Therefore, some possible alterations in Ca^{2+} handling and sarcolemmal ionic currents may have been diminished in cultured cells.

In our study we demonstrated that pseudorabies virus vectors can effectively transduce cultured dog cardiomyocytes. The transferred foreign gene (troponeon) could be detected as early as 16 hours following infection and up to at least four days post-infection. Furthermore, we have shown that infected cardiomyocytes well tolerate the presence of PRV vector, since their electrophysiological properties were not fundamentally changed following the infection. Also, the survival of the cells suitable for electrophysiological studies was high enough even after 4 days, proving that the virus entering the cells did not cause any observable cytotoxic effects; moreover, infected cells displayed largely unaltered electrophysiological properties. This was analyzed by 1) measuring the properties of a specific transmembrane ionic current, the transient outward current (I_{to}), which is known to be ubiquitously present in all ventricular myocytes; 2) analyzing the intracellular Ca^{2+} transient. And verified by FRET measurement the transferred troponeon gene was fully functional. In our study the virus did not affect the I_{to} current (Fig 17). I_{to} was present in all cells even after 72 hours of viral infection, and neither its density nor its kinetics were significantly different from those observed in control cells

(Fig 4). In addition we found that the kinetics of intracellular Ca^{2+} transient was neither significantly different between infected and non-infected cells (Fig 5, 6).

Interestingly, infected myocytes had a lower rate of physiological degradation than non-infected control cells. One possible explanation for this unexpected result is that the delayed apoptosis that may occur in cultured adult cardiomyocytes was further delayed by the viral infection probably through inactivation of the caspase system [61]. Recent studies have suggested that the latency-associated transcript (LAT) region of herpes simplex virus type 1 (HSV-1) is effective at blocking virus-induced apoptosis in vitro in various cell types [62, 63]. Alternatively, it is also possible that Ca^{2+} depletion due to the overexpression of a Ca^{2+}-binding protein (troponeon) resulted in lower cytoplasmic free Ca^{2+} concentrations, which may have anti-apoptotic effects [64].

7. CONCLUSIONS AND FUTURE PERSPECTIVES

In conclusion, using our animal model of type I diabetes mellitus, we were able to reproduce the major characteristic alterations of the myocardial Ca^{2+} handling seen in diabetic patients, such as decreased force of contraction and deteriorated adaptation of the Ca^{2+} cycling in different experimental circumstances. Regarding the underlying mechanisms, we could demonstrate that, depending on the specific circumstances, the decreased SERCA and/or NCX function can play a significant role in these alterations. The moderate alterations that we generally saw in this model belong to the limitations of our study, together with the imperfection of the pharmacological NCX inhibition. Concerning this latter point, however, we demonstrated that SEA0400, the most widely used NCX inhibitor, can be applied when the experimental purpose does not require full NCX blockade. In many cases interpretation of our results invokes careful speculations, which underlines the need of development of more sophisticated Ca^{2+} imaging techniques, with which we can address more specific problems in the Ca^{2+} handling research. As a first step in this direction, we developed and tested a viral vector based gene delivery system that can be a useful tool in studying localized Ca^{2+} signals and other subcellular events or introduce siRNA for silencing ionic channel subunits underlying transmembrane ionic currents, helping to understand disease process at subcellular level in various pathological states, including diabetes.

8. REFERENCES

1. Tsien, R.Y., T. Pozzan, and T.J. Rink, *Calcium homeostasis in intact lymphocytes: cytoplasmic free calcium monitored with a new, intracellularly trapped fluorescent indicator.* J Cell Biol, 1982. **94**(2): p. 325-34.
2. Bers, D.M., *Calcium cycling and signaling in cardiac myocytes.* Annu Rev Physiol, 2008. **70**: p. 23-49.
3. Bers, D.M., *Calcium fluxes involved in control of cardiac myocyte contraction.* Circ Res, 2000. **87**(4): p. 275-81.
4. Bers, D.M., *Cardiac excitation-contraction coupling.* Nature, 2002. **415**(6868): p. 198-205.
5. Bers, D.M., *Cardiac Na/Ca exchange function in rabbit, mouse and man: what's the difference?* J Mol Cell Cardiol, 2002. **34**(4): p. 369-73.
6. Fein, F.S., *Diabetic cardiomyopathy.* Diabetes Care, 1990. **13**(11): p. 1169-79.
7. Bouchard, R.A. and D. Bose, *Influence of experimental diabetes on sarcoplasmic reticulum function in rat ventricular muscle.* Am J Physiol, 1991. **260**(2 Pt 2): p. H341-54.
8. Lagadic-Gossmann, D., et al., *Altered Ca^{2+} handling in ventricular myocytes isolated from diabetic rats.* Am J Physiol, 1996. **270**(5 Pt 2): p. H1529-37.
9. Boudina, S. and E.D. Abel, *Diabetic cardiomyopathy revisited.* Circulation, 2007. **115**(25): p. 3213-23.
10. Grynkiewicz, G., M. Poenie, and R.Y. Tsien, *A new generation of Ca^{2+} indicators with greatly improved fluorescence properties.* J Biol Chem, 1985. **260**(6): p. 3440-50.
11. Minta, A., J.P. Kao, and R.Y. Tsien, *Fluorescent indicators for cytosolic calcium based on rhodamine and fluorescein chromophores.* J Biol Chem, 1989. **264**(14): p. 8171-8.
12. Gee, K.R., et al., *Chemical and physiological characterization of fluo-4 $Ca(^{2+})$-indicator dyes.* Cell Calcium, 2000. **27**(2): p. 97-106.
13. Paredes, R.M., et al., *Chemical calcium indicators.* Methods, 2008. **46**(3): p. 143-51.
14. Prasher, D.C., et al., *Primary structure of the Aequorea victoria green-fluorescent protein.* Gene, 1992. **111**(2): p. 229-33.
15. Chalfie, M., et al., *Green fluorescent protein as a marker for gene expression.* Science, 1994. **263**(5148): p. 802-5.
16. Inouye, S. and F.I. Tsuji, *Aequorea green fluorescent protein. Expression of the gene and fluorescence characteristics of the recombinant protein.* FEBS Lett, 1994. **341**(2-3): p. 277-80.
17. Miyawaki, A., et al., *Fluorescent indicators for Ca^{2+} based on green fluorescent proteins and calmodulin.* Nature, 1997. **388**(6645): p. 882-7.
18. Griesbeck, O., et al., *Reducing the environmental sensitivity of yellow fluorescent protein. Mechanism and applications.* J Biol Chem, 2001. **276**(31): p. 29188-94.
19. Miyawaki, A., et al., *Dynamic and quantitative Ca^{2+} measurements using improved cameleons.* Proc Natl Acad Sci U S A, 1999. **96**(5): p. 2135-40.

20. Heim, N. and O. Griesbeck, *Genetically encoded indicators of cellular calcium dynamics based on troponin C and green fluorescent protein.* J Biol Chem, 2004. **279**(14): p. 14280-6.
21. Takahashi, A., et al., *Measurement of intracellular calcium.* Physiol Rev, 1999. **79**(4): p. 1089-125.
22. Palmer, A.E. and R.Y. Tsien, *Measuring calcium signaling using genetically targetable fluorescent indicators.* Nat Protoc, 2006. **1**(3): p. 1057-65.
23. Shuai, J. and I. Parker, *Optical single-channel recording by imaging Ca^{2+} flux through individual ion channels: theoretical considerations and limits to resolution.* Cell Calcium, 2005. **37**(4): p. 283-99.
24. Melo, L.G., et al., *Gene and cell-based therapies for heart disease.* FASEB J, 2004. **18**(6): p. 648-63.
25. Ly, H., et al., *Gene therapy in the treatment of heart failure.* Physiology (Bethesda), 2007. **22**: p. 81-96.
26. Guzman, R.J., et al., *Efficient gene transfer into myocardium by direct injection of adenovirus vectors.* Circ Res, 1993. **73**(6): p. 1202-7.
27. Donahue, J.K., et al., *Ultrarapid, highly efficient viral gene transfer to the heart.* Proc Natl Acad Sci U S A, 1997. **94**(9): p. 4664-8.
28. Schulick, A.H., et al., *In vivo gene transfer into injured carotid arteries. Optimization and evaluation of acute toxicity.* Circulation, 1995. **91**(9): p. 2407-14.
29. Poller, W., et al., *Highly variable expression of virus receptors in the human cardiovascular system. Implications for cardiotropic viral infections and gene therapy.* Z Kardiol, 2002. **91**(12): p. 978-91.
30. Nalbantoglu, J., et al., *Expression of the primary coxsackie and adenovirus receptor is downregulated during skeletal muscle maturation and limits the efficacy of adenovirus-mediated gene delivery to muscle cells.* Hum Gene Ther, 1999. **10**(6): p. 1009-19.
31. Maeda, Y., et al., *Efficient gene transfer into cardiac myocytes using adeno-associated virus (AAV) vectors.* J Mol Cell Cardiol, 1998. **30**(7): p. 1341-8.
32. Du, L., et al., *Differential myocardial gene delivery by recombinant serotype-specific adeno-associated viral vectors.* Mol Ther, 2004. **10**(3): p. 604-8.
33. Sakoda, T., et al., *A high-titer lentiviral production system mediates efficient transduction of differentiated cells including beating cardiac myocytes.* J Mol Cell Cardiol, 1999. **31**(11): p. 2037-47.
34. Zhao, J., et al., *Lentiviral vectors for delivery of genes into neonatal and adult ventricular cardiac myocytes in vitro and in vivo.* Basic Res Cardiol, 2002. **97**(5): p. 348-58.
35. Boldogkoi, Z., et al., *Pseudorabies virus-based gene delivery to rat embryonic spinal cord grafts.* Hum Gene Ther, 2002. **13**(6): p. 719-29.
36. Boldogkoi, Z., et al., *Novel tracing paradigms--genetically engineered herpesviruses as tools for mapping functional circuits within the CNS: present status and future prospects.* Prog Neurobiol, 2004. **72**(6): p. 417-45.
37. Boldogkoi, Z., et al., *Genetically timed, activity-sensor and rainbow transsynaptic viral tools.* Nat Methods, 2009.

38. Lengyel, C., et al., *Role of slow delayed rectifier K^+-current in QT prolongation in the alloxan-induced diabetic rabbit heart.* Acta Physiol (Oxf), 2008. **192**(3): p. 359-68.
39. Shimoni, Y., H.S. Ewart, and D. Severson, *Type I and II models of diabetes produce different modifications of K^+ currents in rat heart: role of insulin.* J Physiol, 1998. **507 (Pt 2)**: p. 485-96.
40. Shimoni, Y., et al., *Modulation of potassium currents by angiotensin and oxidative stress in cardiac cells from the diabetic rat.* J Physiol, 2005. **567**(Pt 1): p. 177-90.
41. Birinyi, P., et al., *Effects of SEA0400 and KB-R7943 on Na^+/Ca^{2+} exchange current and L-type Ca^{2+} current in canine ventricular cardiomyocytes.* Naunyn Schmiedebergs Arch Pharmacol, 2005. **372**(1): p. 63-70.
42. Fowler, M.R., et al., *Complex modulation of L-type Ca($^{2+}$) current inactivation by sorcin in isolated rabbit cardiomyocytes.* Pflugers Arch, 2009. **457**(5): p. 1049-60.
43. Restrepo, J.G. and A. Karma, *Spatiotemporal intracellular calcium dynamics during cardiac alternans.* Chaos, 2009. **19**(3): p. 037115.
44. Acsai, K., et al., *Effect of partial blockade of the Na($^+$)/Ca($^{2+}$)-exchanger on Ca($^{2+}$) handling in isolated rat ventricular myocytes.* Eur J Pharmacol, 2007. **576**(1-3): p. 1-6.
45. Farkas, A.S., et al., *Na($^+$)/Ca($^{2+}$) exchanger inhibition exerts a positive inotropic effect in the rat heart, but fails to influence the contractility of the rabbit heart.* Br J Pharmacol, 2008. **154**(1): p. 93-104.
46. Ozdemir, S., et al., *Pharmacological inhibition of na/ca exchange results in increased cellular Ca^{2+} load attributable to the predominance of forward mode block.* Circ Res, 2008. **102**(11): p. 1398-405.
47. Birinyi, P., et al., *The Na^+/Ca^{2+} exchange blocker SEA0400 fails to enhance cytosolic Ca^{2+} transient and contractility in canine ventricular cardiomyocytes.* Cardiovasc Res, 2008. **78**(3): p. 476-84.
48. Lengyel, C., et al., *Diabetes mellitus attenuates the repolarization reserve in mammalian heart.* Cardiovasc Res, 2007. **73**(3): p. 512-20.
49. Adachi-Akahane, S., et al., *Calcium signaling in transgenic mice overexpressing cardiac Na($^+$)-Ca^{2+} exchanger.* J Gen Physiol, 1997. **109**(6): p. 717-29.
50. Chossat, N., et al., *Adenoviral SERCA1a gene transfer to adult rat ventricular myocytes induces physiological changes in calcium handling.* Cardiovasc Res, 2001. **49**(2): p. 288-97.
51. Pohlmann, L., et al., *Cardiac myosin-binding protein C is required for complete relaxation in intact myocytes.* Circ Res, 2007. **101**(9): p. 928-38.
52. Rinne, A., et al., *Gene silencing in adult rat cardiac myocytes in vitro by adenovirus-mediated RNA interference.* J Muscle Res Cell Motil, 2006. **27**(5-7): p. 413-21.
53. Communal, C., et al., *Decreased efficiency of adenovirus-mediated gene transfer in aging cardiomyocytes.* Circulation, 2003. **107**(8): p. 1170-5.
54. Li, Z., et al., *Adenovirus-mediated gene transfer to adult mouse cardiomyocytes is selectively influenced by culture medium.* J Gene Med, 2003. **5**(9): p. 765-72.
55. Liu, X., et al., *Silencing GIRK4 expression in human atrial myocytes by adenovirus-delivered small hairpin RNA.* Mol Biol Rep, 2009. **36**(6): p. 1345-52.
56. Himmel, H.M., et al., *Four different components contribute to outward current in rat ventricular myocytes.* Am J Physiol, 1999. **277**(1 Pt 2): p. H107-18.

57. Jost, N., et al., *Restricting excessive cardiac action potential and QT prolongation: a vital role for IKs in human ventricular muscle.* Circulation, 2005. **112**(10): p. 1392-9.
58. Radicke, S., et al., *Functional modulation of the transient outward current Ito by KCNE beta-subunits and regional distribution in human non-failing and failing hearts.* Cardiovasc Res, 2006. **71**(4): p. 695-703.
59. Lipp, P., et al., *Spatially non-uniform Ca^{2+} signals induced by the reduction of transverse tubules in citrate-loaded guinea-pig ventricular myocytes in culture.* J Physiol, 1996. **497 (Pt 3)**: p. 589-97.
60. Viero, C., et al., *A primary culture system for sustained expression of a calcium sensor in preserved adult rat ventricular myocytes.* Cell Calcium, 2008. **43**(1): p. 59-71.
61. Communal, C., et al., *Functional consequences of caspase activation in cardiac myocytes.* Proc Natl Acad Sci U S A, 2002. **99**(9): p. 6252-6.
62. Ahmed, M., et al., *Regions of the herpes simplex virus type 1 latency-associated transcript that protect cells from apoptosis in vitro and protect neuronal cells in vivo.* J Virol, 2002. **76**(2): p. 717-29.
63. Inman, M., et al., *Region of herpes simplex virus type 1 latency-associated transcript sufficient for wild-type spontaneous reactivation promotes cell survival in tissue culture.* J Virol, 2001. **75**(8): p. 3636-46.
64. Chen, X., et al., *Ca^{2+} influx-induced sarcoplasmic reticulum Ca^{2+} overload causes mitochondrial-dependent apoptosis in ventricular myocytes.* Circ Res, 2005. **97**(10): p. 1009-17.

9. ACKNOWLEDGEMENTS

I am very grateful to Professor András Varró, MD, DSc, for his continuous support and for providing me the opportunity for research at the Department of Pharmacology and Pharmacotherapy and to Professor Gyula Papp MD, DSc, academician for his criticism and helpful advice.

I am especially thankful to my supervisors András Tóth, PhD, for his continuous support and personal guidance at the Department of Pharmacology and Pharmacotherapy and for introducing me to the fluorescent techniques. His personal guidance and helpful discussions were useful during my work and allowed me to learn the critical thinking in the scientific field. My special thanks are due to Professor Zsolt Boldogköi for his dedicated support for my first publication.

I wish to thank my grateful colleague, Károly Acsai PhD, for his continuous support and help to study the experimental techniques in the field of the electrophysiology, and I wish to thank Balázs Ördög PhD for his many exceptionally useful help and piece of advice in my molecular works.

I would like to thank all my direct colleagues, Norbert Nagy PhD; Zoltán Márton PhD; Anita Kormos; and to Judit Szepesi for their help in my work. I am also very thankful to Zsuzsanna Sebők for her helpful technical assistance.

A particular acknowledgement goes to my parents, brother, sister, and all my friends for their help and encouragement, to whom I dedicated this PhD thesis. Finally, my deepest appreciation goes to my dear love, Piroska, for her love, support and encouragement in the past years.

10. ANNEX

Publications related to the subject of the Thesis.